UNIVERSIDADE FEDERAL DE MINAS GERAIS
INSTITUTO DE GEOCIÊNCIAS
PROGRAMA DE PÓS-GRADUAÇÃO EM GEOLOGIA

DISSERTAÇÃO DE MESTRADO

CARACTERIZAÇÃO FACIOLÓGICA, PETROGRÁFICA E GEOQUÍMICA DE CONDUTO VULCÂNICO DA FORMAÇÃO SERRA GERAL NA BARRAGEM DE ÁGUA VERMELHA, DIVISA MG/SP

AUTOR: Fernando Estevão Rodrigues Crincoli Pacheco

ORIENTAÇÃO: Fabrício de Andrade Caxito

CO-ORIENTAÇÃO: Lúcia Castanheira de Moraes

Nº 174

BELO HORIZONTE

DATA (18/05/2017)

FERNANDO ESTEVÃO RODRIGUES CRINCOLI PACHECO

CARACTERIZAÇÃO FACIOLÓGICA, PETROGRÁFICA E GEOQUÍMICA DE CONDUTO VULCÂNICO DA FORMAÇÃO SERRA GERAL NA BARRAGEM DE ÁGUA VERMELHA, DIVISA MG/SP

Instituto de Geociências

Dissertação apresentada ao programa de Pós- Graduação em Geologia do Instituto de Geociências da Universidade Federal de Minas Gerais como requisito para a obtenção do título de Mestre em Geologia.

Área de Concentração: Geologia Regional

Orientador: Prof. Dr. Fabrício Andrade Caxito

Co-orientador: Profa. Dra. Lúcia Castanheira de Moraes

Belo Horizonte - MG
2017

P116c
2017

Pacheco, Fernando Estevão Rodrigues Crincoli.

Caracterização faciológica, petrográfica e geoquímica de conduto vulcânico da Formação Serra Geral, na Barragem de Água Vermelha, divisa MG/SP [manuscrito] / Fernando Estevão Rodrigues Crincoli Pacheco. – 2017.

vii, 63 f., enc. (principalmente color.)

Orientador: Fabrício Andrade Caxito.

Coorientadora: Lúcia Castanheira de Moraes.

Dissertação (mestrado) – Universidade Federal de Minas Gerais, Instituto de Geociências, 2017.

Área de concentração: Geologia Regional.

Bibliografia: f. 55-63.

1. Rochas ígneas – Minas Gerais – Teses. 2. Rochas ígneas – São Paulo – Teses. 3. Petrologia – Teses. 4. Geoquímica – Teses. 5. Fácies (Geologia) – Teses. I. Caxito, Fabrício de Andrade. II. Moraes, Lúcia Castanheira de. III. Universidade Federal de Minas Gerais. Instituto de Geociências. IV. Título.

CDU: 552.3(815.1+815.6)

Ficha catalográfica elaborada pela Biblioteca do Instituto de Geociências - UFMG

UNIVERSIDADE FEDERAL DE MINAS GERAIS

PROGRAMA DE PÓS-GRADUAÇÃO EM GEOLOGIA

FOLHA DE APROVAÇÃO

CARACTERIZAÇÃO FACIOLÓGICA, PETROGRÁFICA E GEOQUÍMICA DE CONDUTO VULCÂNICO DA FORMAÇÃO SERRA GERAL NA BARRAGEM DE ÁGUA VERMELHA, DIVISA MG/SP

FERNANDO ESTÊVÃO RODRIGUES CRINCOLI PACHECO

Dissertação submetida à Banca Examinadora designada pelo Colegiado do Programa de Pós-Graduação em GEOLOGIA, como requisito para obtenção do grau de Mestre em GEOLOGIA, área de concentração GEOLOGIA REGIONAL.

Aprovada em 18 de maio de 2017, pela banca constituída pelos membros:

Prof(a). Fabricio de Andrade Caxito - Orientador
UFMG

Prof(a). Patricia Barbosa de Albuquerque Sgarbi
UFMG

Prof(a). Glaucia Nascimento Queiroga
UFOP

Belo Horizonte, 18 de maio de 2017.

AGRADECIMENTOS

Agradeço ao meu orientador, Prof. Dr. Fabrício de Andrade Caxito, e minha co-orientadora, Profa. Dra. Lúcia Castanheira de Moraes, por todo o suporte intelectual, prático e emocional oferecido ao longo dessa trajetória. Vocês foram fundamentais para que este trabalho fosse desenvolvido e eu agradeço de coração pela oportunidade concedida.

Agradeço às amigas, Janaína e Eliza, por me motivarem a ingressar no mestrado. Agradeço também a Paula, minha amiga e companheira de estudos, que esteve ao meu lado durante todo o processo para ingressar no mestrado e durante toda a caminhada que fizemos juntos. Agradeço aos amigos Tobias, Christopher e Carolina pelo companheirismo ao longo de nossa trajetória. Creio que tivemos discussões excelentes, sempre contribuindo para o desenvolvimento de nossos trabalhos.

Agradeço ao Prof. Dr. Hildor Seer por todo o suporte no trabalho de campo de reconhecimento da área do mestrado.

Agradeço aos meus pais e ao meu irmão pelo apoio, incentivo e confiança ao longo de todos esses anos.

Agradeço a Victor pelo apoio incondicional, por estar sempre ao meu lado, me motivando a seguir em frente sempre. Você foi fundamental para o desenvolvimento do processo.

Agradeço ao projeto de mapeamento do Triângulo Mineiro, parceria entre a Companhia de Desenvolvimento Econômico de Minas Gerais (CODEMIG) em colaboração com o Centro de Pesquisa Manoel Teixeira da Costa (CPMTC-UFMG), pelo apoio financeiro. Aos professores Yara Regina Marangoni e Roberto Paulo Zanon dos Santos e ao projeto FAPESP 2012/06082-6, pelas análises geofísicas e parceria no trabalho submetido à revista Journal of Volcanology and Geothermal Researches. Ao Conselho Nacional de Desenvolvimento Científico e Tecnológico (CNPq) pela bolsa concedida. Aos revisores da revista Journal of Volcanology and Geothermal Researches e da revista Brazilian Journal of Geology pelos comentários e sugestões ao artigo submetido.

RESUMO

Este trabalho disserta sobre uma estrutura circular em basaltos da Formação Serra Geral, localizada no leito do Rio Grande entre as cidades de Iturama (MG) e Ouroeste (SP) e será apresentado na forma de dois artigos. O primeiro artigo apresenta o mapeamento geológico na escala 1:1.000, com análises estratigráfica, gravimétrica e petrográfica da estrutura circular em basalto mais preservada na região. O derrame central apresenta basalto rico em vesículas e amígdalas, spatter e estruturas de corda e degaseificação. O nível basal é composto por basalto maciço com geodos preenchidos por quartzo ou basalto. Os demais derrames são maciços, com disjunções colunares, onde foi possível identificar o contato topo e base e apresentam mergulhos suaves para o exterior da estrutura. Uma proeminente estrutura de diques de forma anelar mergulha em direção ao lago de lava apresenta disjunções colunares horizontais e corta os derrames basal e central. Análise gravimétrica mostra uma anomalia Bouguer negativa e fraca no centro da estrutura circular. O modelo proposto para o vulcanismo na região segue três etapas principais: (1) ocorrência de derrame fissural com fluxo de lava; (2) essa lava resfria e cristaliza ao longo da maior parte da fissura, promovendo a formação de condutos centrais localizados; e (3) ocorrem fraturas anelares e radiais ao redor do lago de lava devido à presença de gases dissolvidos. O magma usa algumas dessas fissuras anelares para a extrusão e os derrames se tornam diques na forma anelar das fraturas. O segundo artigo apresenta análises detalhadas de petrografia, litoquímica e química mineral. Os basaltoss da estrutura circular foram divididos em quarto grupos (central flow, basal flow, main ring dyke and lava flow), baseado em texturas e estruturas, e apresentam uma petrográfica muito similar, composta por plagioclásio (labradorita-bytownita), clinopiroxênio (augita) e óxido (titanomagnetita), com textura intergranular. A analyses geoquímica de rocha total do basal e lava flows permitiram a sua classificação como basaltos toleíticos do tipo Paranapanema. A interpretação de dados geoquímicos sugerem uma fonte mantélica enriquecida, com baixo grau de fusão parcial e alta profundidade de geração de melt, sem uma contaminação crustal significante. Os basaltos da estrutura circular sofreram cristalização fracionada em uma câmara magmática superficial e foi incluenciada pela injeção de novos magmas responsáveis por pulsos de efusão e explosão. Assim, as singularidades da estrutura circular dos basaltos de Água Vermelha são importantes para a compreensão da evolução da Província Magmática Paraná-Etendeka.

Palavras-chave: Formação Serra Geral; Província Magmática Paraná-Etendeka; Estrutura Circular; litoquímica; química mineral; petrografia

ABSTRACT

This work shows information about a basaltic ring structure (BRS) of Serra Geral Formation, localized on Rio Grande riverbed between the cities of Iturama (MG) and Ouroeste (SP) and is going to be presented in the form of two papers. The first one shows a detailed geological mapping at 1:1000 scale, stratigraphic, petrographic and gravimetric analysis of the most well preserved of the BRS. The central flow, interpreted as a preserved lava lake, comprises basalt rich in vesicles and amygdales, spatters, ropy and degassing structures. The basal flow has massive basalt containing geodes filled with quartz or basalt. Above, the lava flows show massive basalt with vertical columnar jointing where is possible to identify the top and bottom of each individual flow, with gentle dips towards the perimeter of the structure. A prominent ring dyke dipping towards the lava lake presents horizontal columnar jointing and cuts the basal and central flows. The gravimetric analysis shows a weak negative Bouguer anomaly on the center of the BRS. The proposed model describes the volcanism of the region in three main steps: (1) fissure flow occurs with lava input; (2) this lava cools and crystallises cementing most of the fissures, promoting the formation of localized central conduits; and (3) the presence of dissolved gas in lava produces ring and radial fractures around the solidified lava lake. The magma uses some of the ring fissures to ascend and the following lava flows assume the ring shape of the dyke vent. The second one shows detailed analyses of petrography, lithochemistry and mineral chemistry. The BRS rocks, based on textures and structures, were divided into four groups (central flow, basal flow, main ring dyke and lava flow) with a very similar petrography, composed of plagioclase (labradorite-bytownite), clinopyroxene (augite) and oxide (titanomagnetite) with intergranular texture. The whole-rock geochemical analyses of the basal and lava flows allow classifying them as tholeiitic basalts of the Paranapanema magma-type. Geochemical data interpretation suggests an enriched magma source, with low degree of partial melting and high depth of melt generation and without significant crustal contamination. The BRS experienced fractional crystallization on the shallow magma chamber, influenced by new magma injections responsible for the pulses of

effusion and explosion. Thus, the singularities of the BRS of Água Vermelha are important to the comprehension of the evolution of the PEMP.

Keywords: Serra Geral Formation, Magmatic Province Paraná-Etendeka; Basaltic ring structure; lithochemistry; mineral chemistry; petrography

SUMÁRIO

CONSIDERAÇÕES INICIAIS

Esta dissertação consiste nos resultados obtidos ao longo do mestrado do aluno Fernando Estevão Rodrigues Crincoli Pacheco no período de março de 2015 a abril de 2017. Este trabalho teve como principal objetivo a caracterização e interpretação de uma estrutura circular presente na Formação Serra Geral, no leito do Rio Grande entre as cidades de Iturama (MG) e Ouroeste (SP).

A apresentação desse trabalho será na forma de dois artigos. O primeiro "BASALTIC RING STRUCTURES OF THE SERRA GERAL FORMATION AT THE SOUTHERN TRIÂNGULO MINEIRO, ÁGUA VERMELHA REGION, BRAZIL", publicado na revista Journal of Volcanology and Geothermal Research, apresentará os resultados referentes ao mapeamento geológico, à geofísica e ao modelo proposto para a evolução da estrutura circular.

O segundo artigo "GEOCHEMISTRY OF BASALTIC FLOWS FROM A BASALT RING STRUCTURE OF THE SERRA GERAL FORMATION AT ÁGUA VERMELHA DAM, TRIÂNGULO MINEIRO, BRAZIL: IMPLICATIONS FOR THE MAGMATIC EVOLUTION OF THE PARANÁ-ETENDEKA PROVINCE", em fase de revisão, submetido na revista Brazilian Journal of Geology, apresenta os resultados relacionados à petrografia, litoquímica e química mineral. Esses trabalhos foram desenvolvidos com o apoio do Projeto de Mapeamento do Triângulo Mineiro (CODEMIG / CPMTC / UFMG), Projeto FAPESP 2012/06082-6 e CNPq. Em seguida, serão apresentadas as considerações finais que articulam os dois artigos confeccionados.

Artigo 1 – BASALTIC RING STRUCTURES OF THE SERRA GERAL FORMATION AT THE SOUTHERN TRIÂNGULO MINEIRO, ÁGUA VERMELHA REGION, BRAZIL

Fernando Estevão Rodrigues Crincoli Pacheco[1], Fabrício de Andrade Caxito[1], Lúcia Castanheira de Moraes[2], Yara Regina Marangoni[3], Roberto Paulo Zanon dos Santos[3], Antônio Carlos Pedrosa-Soares[1]

[1] Universidade Federal de Minas Gerais, Programa de Pós-Graduação em Geologia, CPMTC-IGC-UFMG, Campus Pampulha, 31270-901 Belo Horizonte, MG. (ferodrigues@live.it; boni@ufmg.br; pedrosa@pq.cnpq.br)

[2] Centro Federal de Educação Tecnológica de Minas Gerais – CEFET MG Av. Ministro Olavo Drummond, 25 - CEP 38180-510 - Bairro São Geraldo - Araxá - MG - Brasil (2013luciam@gmail.com)

[3] Universidade de São Paulo, Instituto de Astronomia, Geofísica e Ciências Atmosféricas, Rua do Matão, 1226, CEP: 05508-090, São Paulo, SP, Brazil. (yaramaran@usp.br, roberto.zanon@iag.usp.br)

1. INTRODUCTION

Continental Magmatic Provinces (CMP) are the most researched Large Igneous Provinces (LIP) around the world (e.g.: Jerram & Widdowson, 2005; White et al., 2009), mostly because of their large exposure areas, in contrast to the less acessible oceanic provinces. Within the CMPs the most common rock types are Continental Flood Basalts (CFB), composed of basaltic sequences of variable composition and, subordinately, intermediary and felsic rocks such as dacites and rhyolites (e.g. Hall, 1987). The CMPs are often related to crustal stretching in divergent settings, thus acting as excellent markers of the breakup and dispersion of paleocontinents. The extrusion of great volumes of magma onto the surface of the Earth can lead also to climatic consequences, such as the transfer of volcanic gases to the atmosphere and their interaction with the biosphere (Victor et al., 2009). Thus, the study of CMPs is important for various fields of research, such as petrology, crustal evolution, past tectonics and paleoclimatic and environmental studies.

In Brazil, the Serra Geral Formation of the Paraná basin comprises more than 90% of the Paraná-Etendeka Magmatic Province and displays some classical elements of a CMP. The basaltic magmatism recorded in this formation occupies circa 1,500,000 km2 with a volume of circa 2,300,000 km3 of predominantly basaltic rocks (Courtillot & Renne, 2003). The age of extrusion of these basalts is defined through Ar-Ar data at around 134.7 ± 1 Ma (Renne et al., 1992; Thiede & Vasconcelos, 2010), which is corroborated by a maximum of four magnetic polarity reversals throughout the whole stratigraphic section (Ernesto et al., 1999). These data suggest a rapid extrusion for the basaltic package as whole, which took less than 1.2 Ma. Recent zircon and baddeleyite U-Pb data (Pinto et al., 2011; Janasi et al., 2011) corroborate these data, with ages around 135 Ma.

It is widely thought that the main extrusion mechanism for this rapid basaltic volcanism is through fissures due to intense crustal fracturing, allowing the ascension of magma. It is common to consider the mafic dyke swarms of Ponta Grossa, Serra do Mar and Florianópolis as related to the Serra Geral Formation, as they are considered as feeders for the basaltic plateaus (Marques & Ernesto, 2004). However, throughout the world, additional feeding mechanisms have been proposed for CFBs. For instance, in some lava flows it is possible to identify circular structures (Basaltic Ring Structures – BRS) that might be interpreted as past shield volcanoes, for example Mount Eccles, Southwestern Australia (Boutakoff, 1952, in Faust, 1975), at the Columbia River Plateau in Southwestern USA (Swanson et al., 1975), in Athabasca Valles, on Mars (Jaeger et al., 2005) and in North Mountain Formation, in Nova Scotia, Canada (Webster et al., 2006). Thus, the study of circular structures related to basaltic flows is fundamental to the comprehension of the models of generation and extrusion of magmas in CMPs.

At the southern portion of the Triângulo Mineiro region of Central Brazil, at the Água Vermelha hydroeletric dam of the Grande river, Minas Gerais / São Paulo states, sub-circular structures have been identified in the Serra Geral Formation basalts. Those are interpreted as central conduits by some authors (Araújo et al., 1977; Araújo, 1982; Araújo & Hasui, 1985), although in other places, the BRS were interpreted as collapse structures (McKee & Stradling, 1970) or as the product of explosions caused by phreatic activity (Hodges, 1978). In this paper, we present new field, stratigraphic and

petrography data of the best exposed of those semi-circular structures, aiming to contribute to a better understanding of the structure and evolution of the basaltic magmatism of the Serra Geral Formation.

2. GEOLOGICAL CONTEXT

The Paraná basin developed upon a crystalline and metasedimentary basement in the southeastern region of the South American platform, which was profoundly affected by tectonic, magmatic and metamorphic events during the Neorproterozoic (ca. 900 – 530 Ma) and shows structural trends oriented predominantly at NNE-NE and NW (Mincato, 2000). The basement control the tectonic, sedimentary and magmatic evolution of the Paraná basin (Mincato, 2000), which developed as a large Phanerozoic syneclise over the recently formed Gondwana Supercontinent. Deposition of the sedimentary-magmatic sequence that filled in the Paraná basin occurred from the Upper Ordovician to the Upper Cretaceous (Milani, 2004) and occupies an area of over 1,500,000 km² (Fig. 1). Throughout this time, the Paraná basin was filled by successive sedimentary episodes. Six second order units (Megasequences) constitute the stratigraphic filling of the basin (Fig. 1), with important hiatus between them (Milani, 1997; 2004).

According to Milani et al. (2007), deposition within the basin started through transtensive subsidence, with the Rio Ivaí Megasequence transitional-glacial-marine sediments followed by subsidence controlled mainly by a regional flexure. A major transgression occurred from a coastal to a marine setting responsible for the Paraná Megasequence, then a glacial episode followed by regression deposited the Gondwana I Megasequence and the continental sediments were responsible for the deposition of Gondwana II Megasequence. The lithostatic compaction and thermal subsidence predominated at the Jurassic and the Gondwana III Megasequence was deposited. This megasequence developed in dry climate conditions, beginning with the Botucatu Formation and followed by Serra Geral Formation. This was succeeded by the continental deposits of the Bauru Megasequence, nowadays considered as deposited in a separated basin (Bauru basin).

The Paraná-Etendeka Magmatic Province (PEMP), of which the Serra Geral Formation represents the preserved part of it throughout the Paraná basin, is part of the

Gondwana III Supersequence and its origin is related to the breakup of Gondwana and the opening of the South Atlantic Ocean (Fig. 1; Milani et al., 2007). According to Milani et al. (2007), the PEMP is expressed through a thick lava cover, mafic dyke swarms that crosscut the whole previous stratigraphic package and sills. This intense volcanism covered most of southern Brazil and parts of Paraguay, Uruguay and Argentina (Marques & Ernesto, 2004).

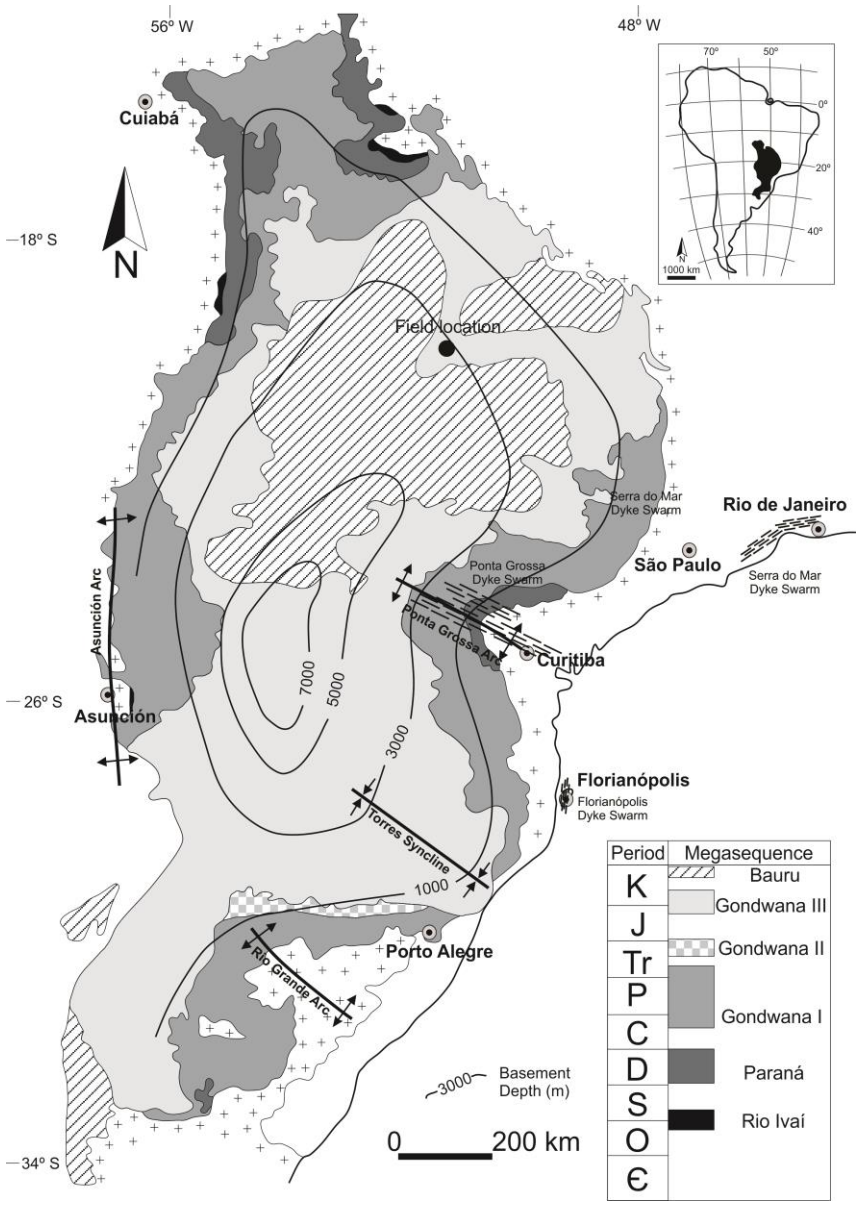

Figure 1 – Simplified geological map of the Paraná basin (adapted from Milani, 2004), with the location of mafic dyke swarms discussed in the text. Solid circle marks the approximate location of the studied area.

The volcanic rocks of Megasequence Gondwana III occur as a thick succession of lava flows, with an average thickness of 650 meters, varying according to the depth of the basin. The lavas are mostly tholeiitic basalts and andesitic basalts, with two

pyroxenes (augite and pigeonite). Subordinately, tholeiitic andesites, rhyodacites and rhyolites occur (Marques & Ernesto, 2004). The latter occurs directly over interdune valleys of the Botucatu Formation (Janasi et al., 2011) or concentrated in the most surficial parts of the flows (Piccirillo & Melfi, 1988, in Marques & Ernesto, 2004). Basaltic rocks are composed of phenocrysts and microphenocrysts (0.2 to 0.5 mm) of plagioclase, augite, pigeonite, lesser titanomagnetite and rare olivine that is variably weathered, in a finer-grained matrix composed by the same minerals (Marques & Ernesto, 2004). Still, according to those authors, volcanism in the PEMP is essentially bimodal (basalt-rhyolite).

The Serra Geral Fomation basaltic rocks have been grouped into six different magma types, being Urubici, Paranapanema and Pitanga the "High-Ti" and Gramado, Ribeira and Esmeralda the "Low-Ti" (Peate et al., 1992). The rhyolitic magma types were divided in the low incompatible element content (Palmas-type) and "rich" incompatible element content (Chapecó-type) (Mantovani et al., 1985, Bellieni et al., 1986). Paranapanema and Pitanga types occur on the entire Paraná basin while the other types are not present on the north of the basin (Fig. 2).

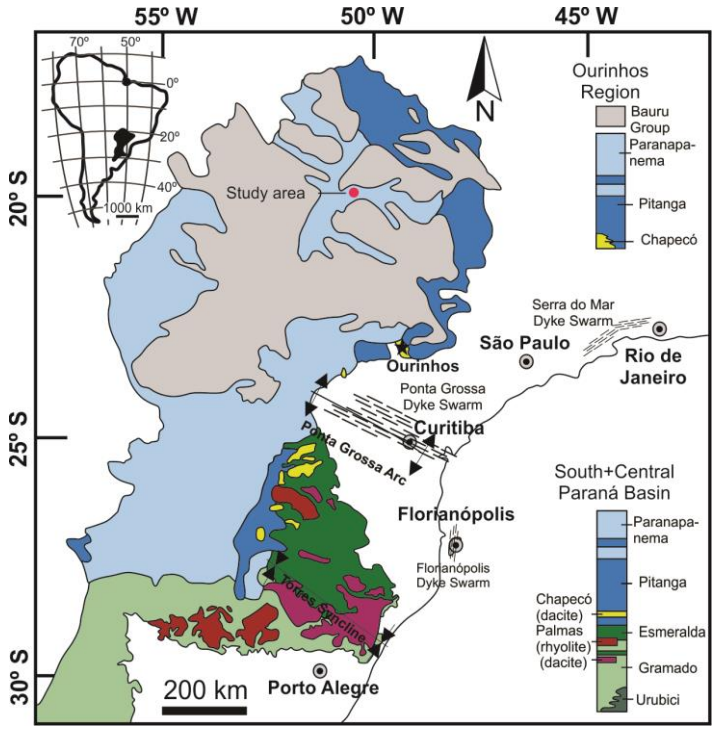

Figure 2 – Map showing the distribution of magma types in the Paraná sedimentary basin (adapted from Janasi et al., 2011), with the location of mafic dyke swarms discussed in the text. Solid red circle marks the approximate location of the studied area.

The PEMP shows an intense intrusive igneous activity represented by many dykes and sills. The dykes are concentrated in the swarms of Ponta Grossa, Serra do Mar and Florianópolis (Fig. 1 and 2). Those dykes are predominantly of basic rocks (diabase), although intermediate to felsic rocks occur sporadically. Those rocks show geochemical characteristics which are similar to the associated volcanic rocks (Bellieni et al., 1984; Piccirillo et al., 1988; Maniesi & Oliveira, 1997; Ernesto et al., 1999).

2.1. The Água Vermelha Region

The Água Vermelha region is located between the towns of Iturama (Minas Gerais state) and Ouroeste (São Paulo state), where a hydroelectric dam was constructed over the Grande riverbed. The geological studies in the region date from the time of construction of the dam, e.g. Araújo et al. (1977), Araújo (1982) and Araújo & Hasui (1985). Basaltic rocks of the Serra Geral Formation in the area occur as both dykes and lava flows. The flows are distributed in conspicuous semi-circular structures, while the dykes are disposed in ring structures (Araújo, 1982).

The lava flows described in the region are characterized by three types of basaltic rocks: basaltic breccias, vesicle-amygdaloidal basalts and massive basalts. The basaltic breccias are restricted and divided in volcanic and pyroclastic. The volcanic type shows angular fragments which are mostly above 64 mm, composed of vesicle-amygdaloidal and massive basalt. The brecciated matrix can be basaltic (generally vesicular), carbonatic or sand-silt. The pyroclastic breccias are formed by angular blocks of vesicle-amygdaloidal and massive basalts cemented by calcite (Araújo & Hasui, 1985). Vesicle-amygdaloidal basalts are characterized by the presence of partially or fully filled amygdales of calcite, quartz, chalcedony, zeolites and clay minerals. The massive basalts, predominant in the region, show a dark gray color, or green to red due to weathering. There is a gradual transition between these latter two types of basalts (Araújo & Hasui, 1985).

The semi-circular structures are expressed in the region as depressions and numbered 1 to 11 in figure 3. They are filled by vesicular-amygdaloidal basalts, with pahoehoe structures, and show a sharp contact with neighboring lava flows or ring dyke. Ring fractures are common (Araújo & Hasui, 1985).

Araújo et al. (1977), Araújo (1982) and Araújo & Hasui (1985) interpret those semi-circular structures as the representation of central conduits. On the other hand, in the Columbia River plateau, similar BRS are interpreted as formed due to the collapse of the roof of very thick lava flows (McKee & Stradling, 1970) or due to phreatic activity (Hodges, 1978). Thus, there is at present a controversy on the nature and significance of those structures. This is a very important issue for the understanding of the dynamics of volcanism in the PEMP.

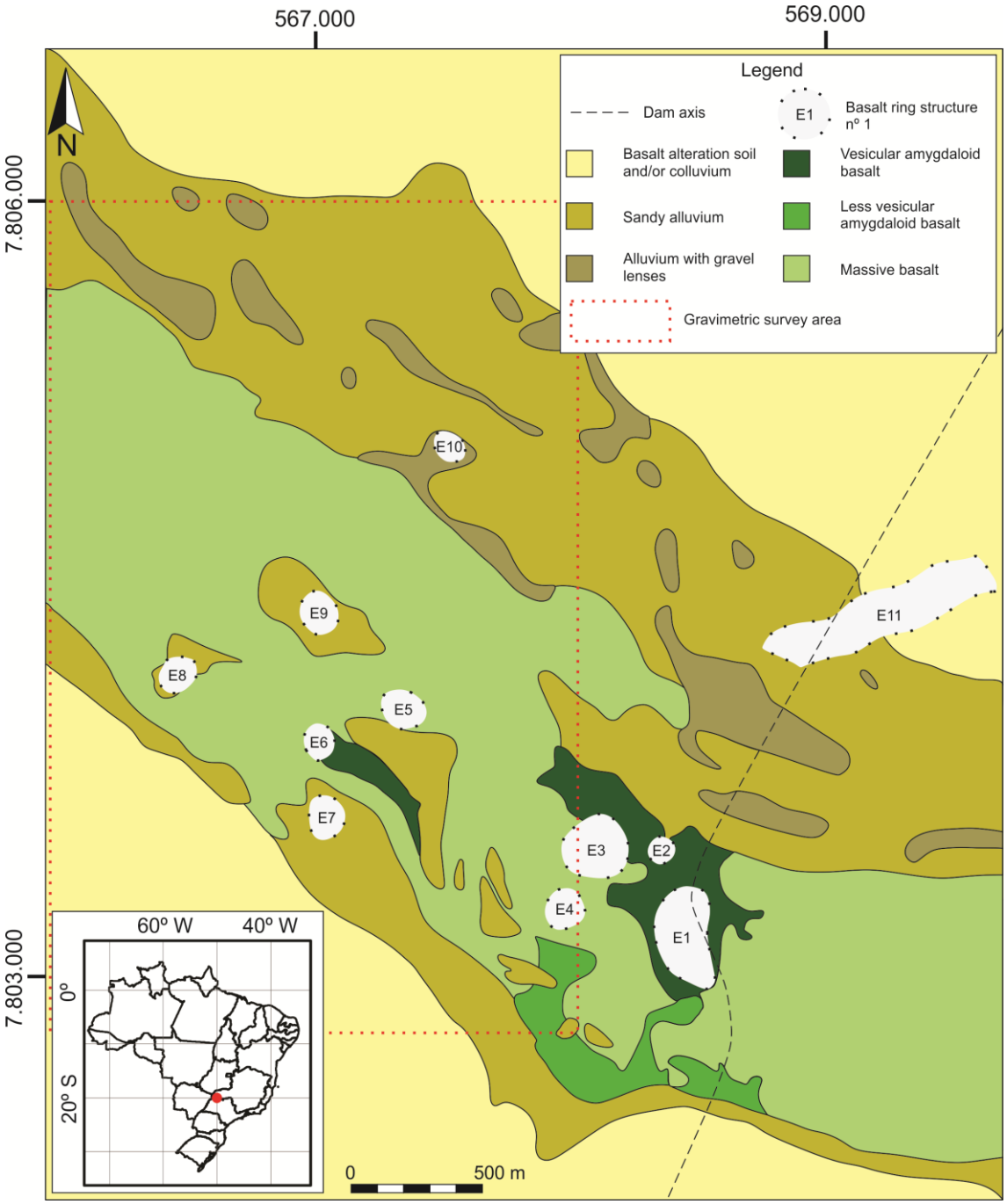

Figure 3 – Geological map of the Água Vermelha region. Adapted from Araújo (1982). The red dots show the area of the gravimetric survey in this article.

3. MATERIALS AND METHODS

In order to provide a better understanding of the ring structures and of the genesis and significance of the lava flows in the Água Vermelha Region, we have mapped in detail the best exposed ring structure (E6 in Fig. 3). 30 samples were collected for petrographic studies in thin section. From the field and satellite imagery data interpreted, a detailed geological map was drawn (Fig. 5) and 13 stratigraphic sections were made (Fig. 6).

We collected 83 gravimetric stations using a LaCoste & Romberg type G gravity meter and a Laica double frequency GPS for coordinates (latitude, longitude and altitude). The survey was done on foot, with GPS carried in the vertical during the survey time. The GPS reduction was done using kinematic procedure and the Brazilian Continuous Monitoring Network (IBGE, 2004). Position data were reduced to WGS-84 system and geometric height was converted in orthometric height using MAPGEO software (IBGE). For the gravimetric survey a local base station was set on Indiaporã town (SP), after a base gravity station transfer from Fernandópolis (SP). Drif and tide, free-air and Bouguer corrections were done using 2670 kg/m3 for density. The gravity model of 1967 was removed from the data. The Complete Bouguer correction was not done due the absence of topographic data. The SRTM for the area was collect when the region was flooded and presents a constant height for the area.

4. RESULTS

The basalts mapped in the E6 structure were divided in flows due to the easily identifiable top and basal sharp contact of each flow (Fig. 4). Those flows are represented in the geological map (Fig. 5) and stratigraphic columns (Fig. 6). Nomenclature of each of the flows follow the numeric order of superposition and lateral continuity. Where it was not possible to determine the lateral correlation of each flow a new sequence was adopted, resulting in two different numberings: 0 to 8 and 1A to 3A; both occur above the basal flow. Dykes crosscut the basalts and in the central flow a vesicular and amygdaloidal basalt which is very distinct from the other flows occur.

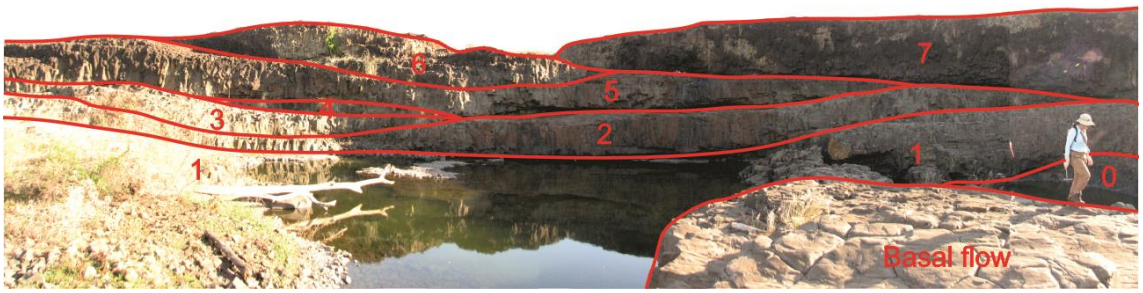

Figure 4 – Lava flows mapped in the southwestern edge of the mapped ring structure. GPS: 7803986 N / 567020 E / Zone 22K / facing southwest.

4.1. Central flow

Composed of gray basalt, orange when weathered, abundant in vesicles and amygdales with an average diameter of 0.5 - 3 cm (Fig. 7A). At some places those vesicles occur as pipes (Fig. 7B) but in general they show no preferential orientation. Amygdales are filled predominantly by calcite and chalcedony or, in a lesser amount, by silica. Pahoehoe structures are common (Fig. 7C) but these show no preferential flow orientantion. This flow presents squeeze up dykes 2 to 10 cm thick (Fig. 7D). It is also possible to identify spatter structures of variable size, milimetric to centimetric, reaching up to 15 cm long (Fig. 7E). Along with the spatters, pipes of degassing structures occur (Fig. 7F).

Petrographically the central flow basalt contains plagioclase and pyroxene laths reaching up to 0.5 mm long, in a vitreous matrix, with abundant vesicles and amygdales (Fig. 7G), filled by zeolites, calcite and chalcedony (Fig. 7H). In the degassing structures it is possible to identify volcanic glass with microphenocrysts of plagioclase and pyroxene reaching up to 1 mm long and zeolite-filled amygdales (Fig. 7I). Thin sections of the spatter show a vitreous matrix surrounding larger crystals of the same minerals. The contact of the spatter structure with the rock matrix is not well defined (Fig. 7J). Devitrification structures are also common. Locally, plagioclase and pyroxene might occur as glomeroporphyries.

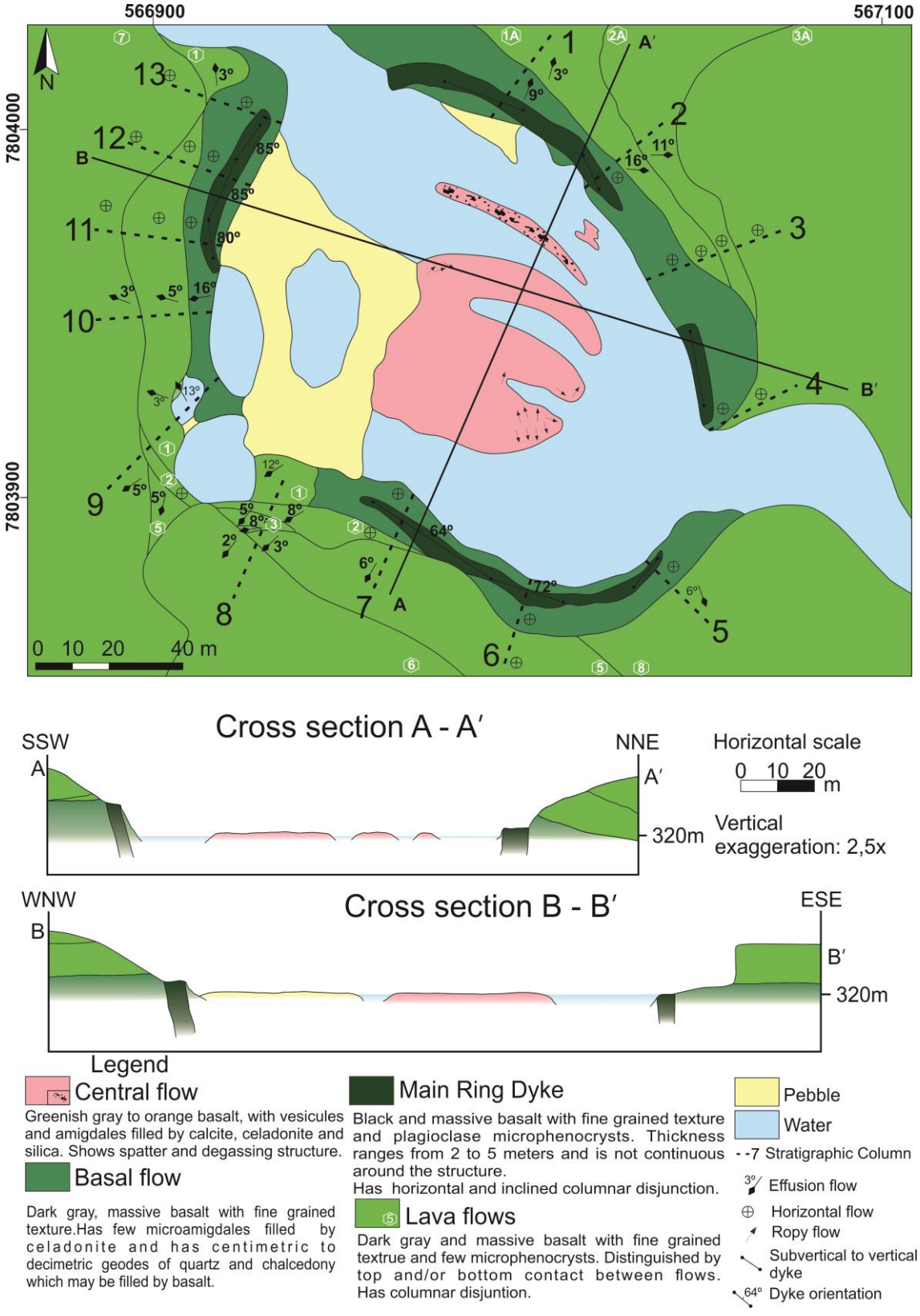

Figure 5- Geological Map of Basalt Ring Structure in Água Vermelha region, MG/SP, Brazil, showing the different basalt flows, structures and location of the studied stratigraphic sections.

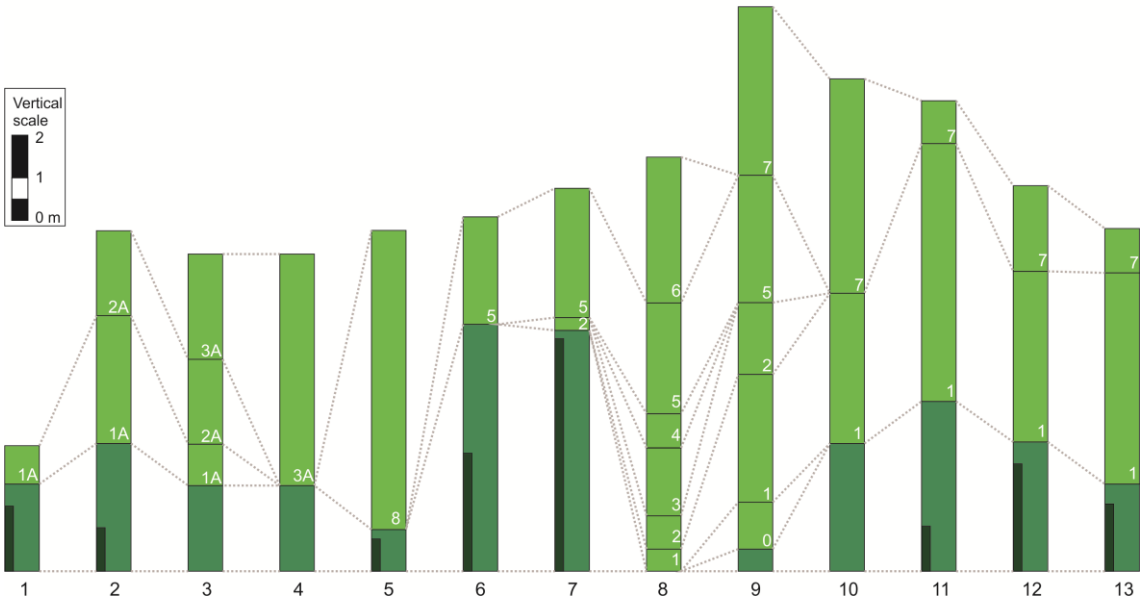

Figure 6 – Stratigraphic section with the representation of basalt flows in ring structure E6. The location of each column is represented in the geological map of Fig. 5 by a dashed line.

4.2. Basal flow

This is composed by homogeneous and massive dark grey basalt, with fine-grained plagioclase and pyroxene. It may rarely show some microamygdales (1 – 2 mm) filled by celadonite, and towards the top of the flow centimetric to decametric geodes occur, reaching up to 60 cm in diameter (Fig. 8A and 8B). Those geodes are filled by quartz and chalcedony, but some are filled with basalt itself. Locally, spheroidal disjunction and gas scape structures also occur. In thin section it is possible to identify microphenocrysts of olivine (Fig. 8C and 8D) and plagioclase (Fig. 8E and 8F) among the plagioclase, pyroxene and volcanic glass matrix.

4.3. Main Ring Dyke

The main ring dyke that occur in structure E6 is shown in the map of Fig. 4. It is composed of black basalt, with a porphyritic texture with microphenocrysts of plagioclase, and the matrix shows a fine- to very fine-grained texture. Its thickness varies from 2 to 5 meters, and it is discontiunous throughout the structure. This ring dyke dips from 64º to ca. 90º, always towards the center of the structure and shows inclined or horizontal columnar joints (Fig. 8G and 8H). In its most external portion near the contact with flow A, in a ca. 50 cm thick belt, there is an intense fracturing perpendicular to the orientation of the columns. In thin sections, it is possible to identify

plagioclase and pyroxene laths, lesser volcanic glass and microamygdales of around 0.5 mm (Fig. 8I and 8J).

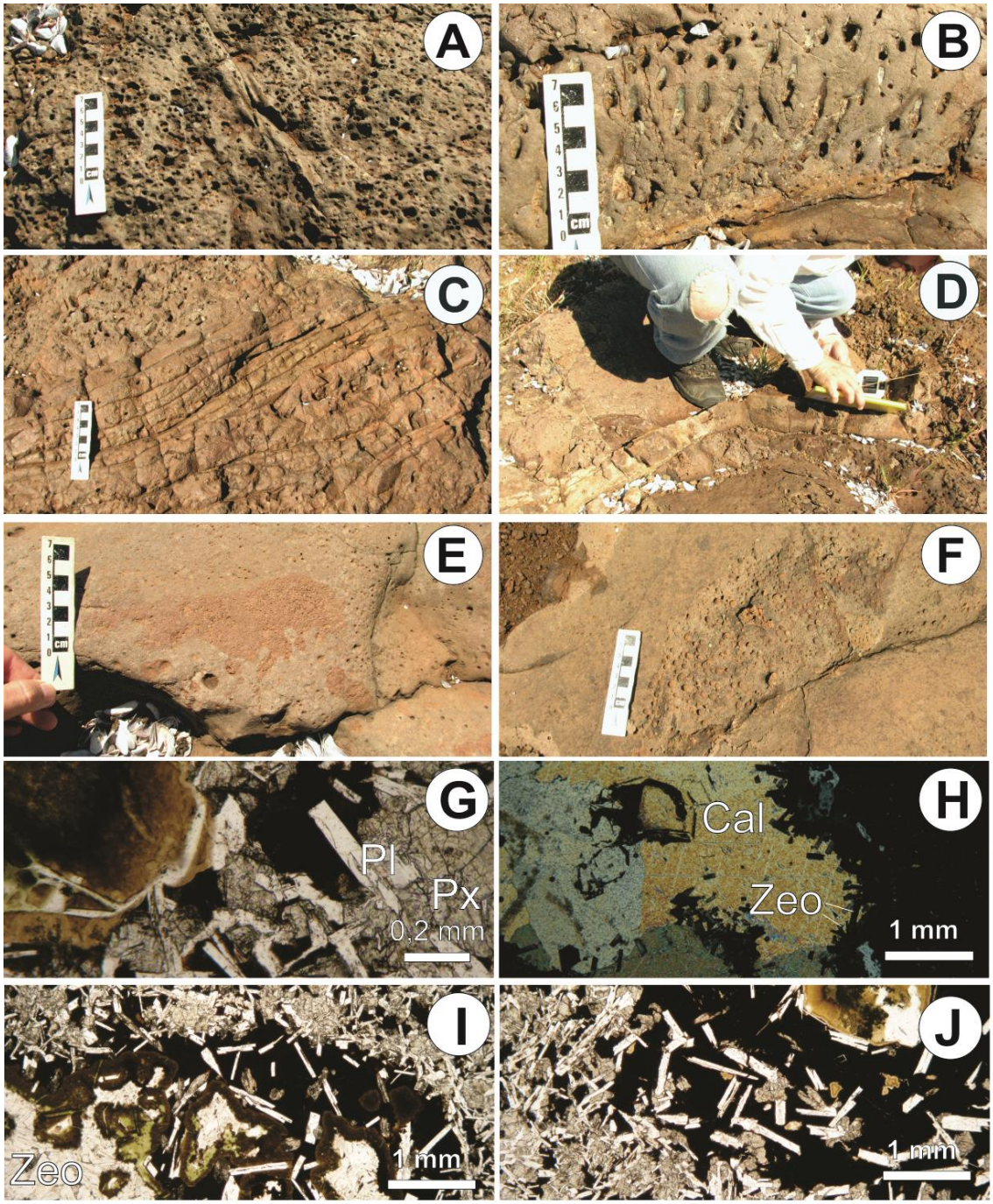

Figure 7 - (A) – central flow basalt, with vesicles and amygdales; (B) – pipes in central flow; (C) – ropy structure; (D) – central flow squeeze up dyke; (E) – spatters; (F) pipe of degassing structure. Photomicrography: (G) – general aspect of the basalt, with plagioclase and pyroxene laths vitreous matrix, plenished with vesicles and amygdales; (H) – amygdale filled by calcite and zeolite, wrapped by glass; (I) – degassing structure with glass wrapping plagioclase and pyroxenes laths and amygdales filled by zeolites; (J) – spatter well-marked by glass and laths, notice the crystal-matrix contact. Px = pyroxene, Pl = plagioclase, Zeo = zeolite, Cal = calcite.

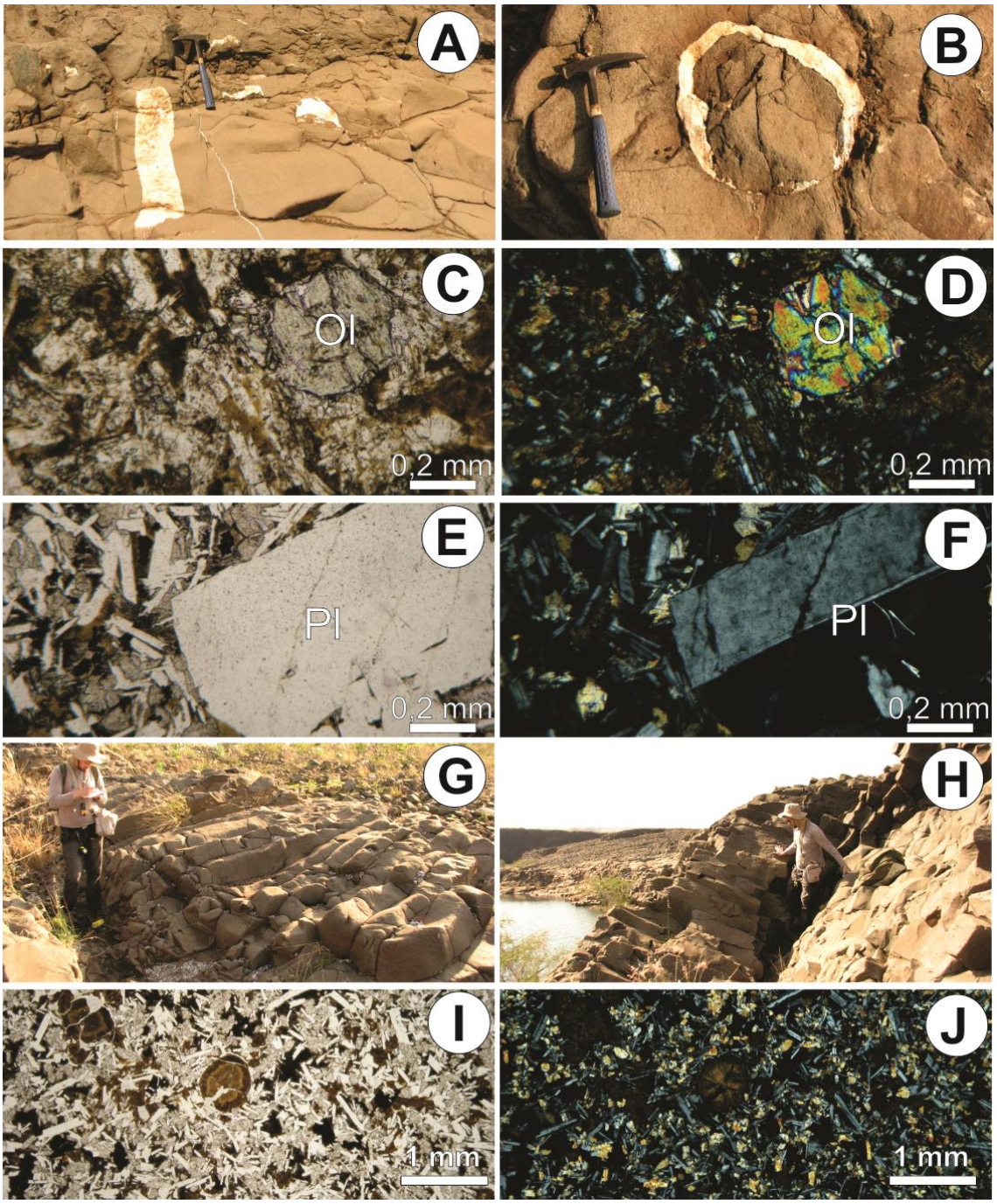

Figure 8 - (A and B) – basal flow general aspect, with quartz geode. Photomicrographies show similar mineralogy to the other flows, with olivine (C and D) and plagioclase microphenocrysts (E and F). Ol = olivine, Pl = plagioclase; (G and H) – basalt dykes with horizontal and inclined columnar disjunction; (I and J) – dyke photomicrography with plagioclase and pyroxene laths, glass and microamygdales.

4.4. 0 – 8 and 1A – 3A Lava Flows

The lava flows are composed by dark grey basalts, with fine phaneritic to aphanitic texture, with rare microphenocrysts. They are separated by sharp top and base contacts (Fig. 4). Those occur above the basal flow and are divided in two continuous stacking series, not easily correlated laterally. The flows are horizontal to sub-

horizontal, sometimes showing gentle dips (up to 16º) towards the external part of the ring structure.

The basalts can show columnar disjunctions, but the central portion is generally massive. At some flows (2, 5) the top show vesicles of up to 0.5 cm, concentrated in 1 - 2 cm thick levels, sometimes aligned in pipes. Microamygdales (1 mm) filled by celadonite were identified (1A and 2A flows). Mineralogically the basalts are composed of laths of plagioclase and pyroxene, showing lesser volcanic glass and microphenocrysts of plagioclase, pyroxene and olivine (Fig. 9A e 9B). Plagioclase may show a concentric (Fig. 9C) or sectorized (hourglass) zoning (Fig. 9D).

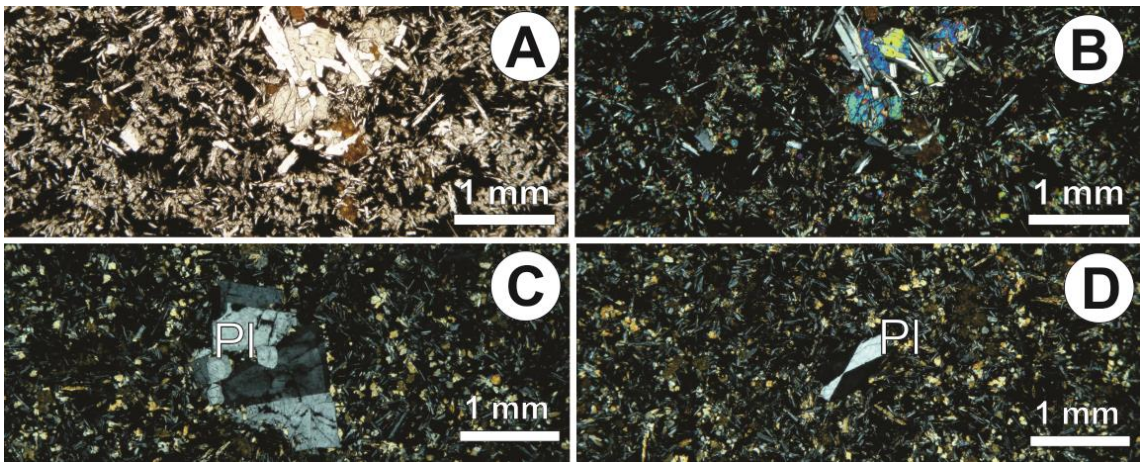

Figure 9 - Figure 9 – (A and B) lava flows photomicrographies, presenting plagioclase and pyroxene microphenocrysts; (C) concentric zoning of plagioclase; (D) sectoring zoning (hourglass) of plagioclase. Pl = plagioclase.

4.5. Gravimetry

The gravimetric survey objective was to observe the gravity response of the structures. Ring structures present gravity anomalies like discussed in Pilkington and Grieve (1992). The area where the gravimetric survey was conducted is marked with red dots and our BRS is the E6 (Fig. 5). As can be seen in the elevation map (Fig. 10) the depressions are 5 to 10 meters below the outside rings. Through the Bouguer anomaly map (Fig. 11) it is possible to identify a regional positive anomaly over the area of Água Vermelha, however, locally, the BRS shows a weak negative anomaly of -0.5 to -1.0 mGal. This negative gravimetric anomaly occurs where the structure has a low topography, as seen on the comparative transections of Bouguer anomaly and altitude (Fig. 12). We have not done terrain correction on the gravimetric data, because we do

not have enough resolution in topography at the moment. In order to do it, with these small topographic differences it is necessary to perform an altimetry survey that is impossible due to usual flooding from the dam. The gravity survey, presented here, was conducted in a rough dry season, after a few years of low rain rates. So, those structures, usually under water, were exposed. The impossibility to perform terrain correction may not put away the possibility that the low Bouguer anomaly is only due to topography.

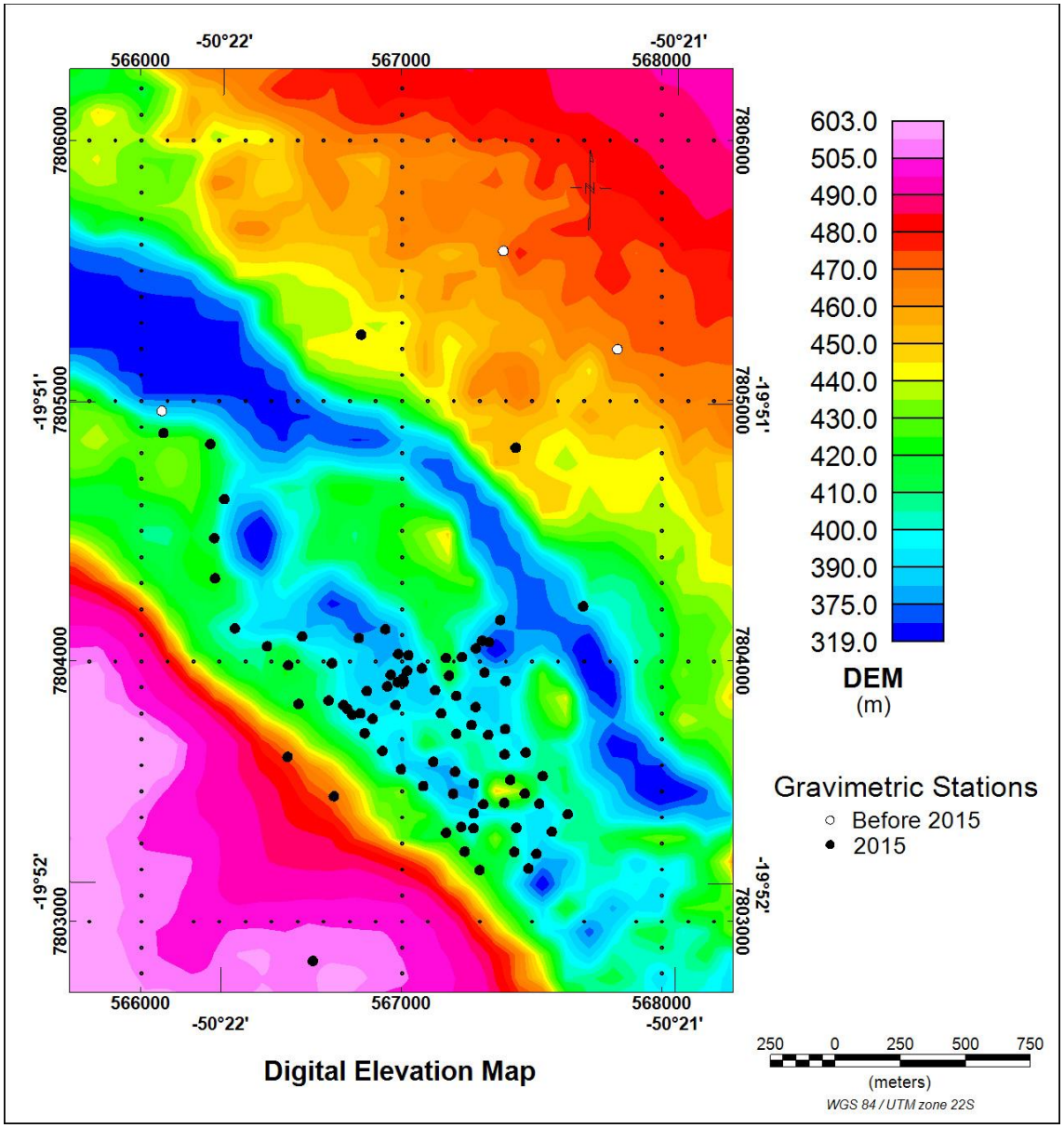

Figure 10 – Terrain elevation map obtained from SRTM90 digital model, and location of gravimetric points (black for 2015 survey and white for previous regional surveys). SRTM90 resolution is of 90 m at the equator.

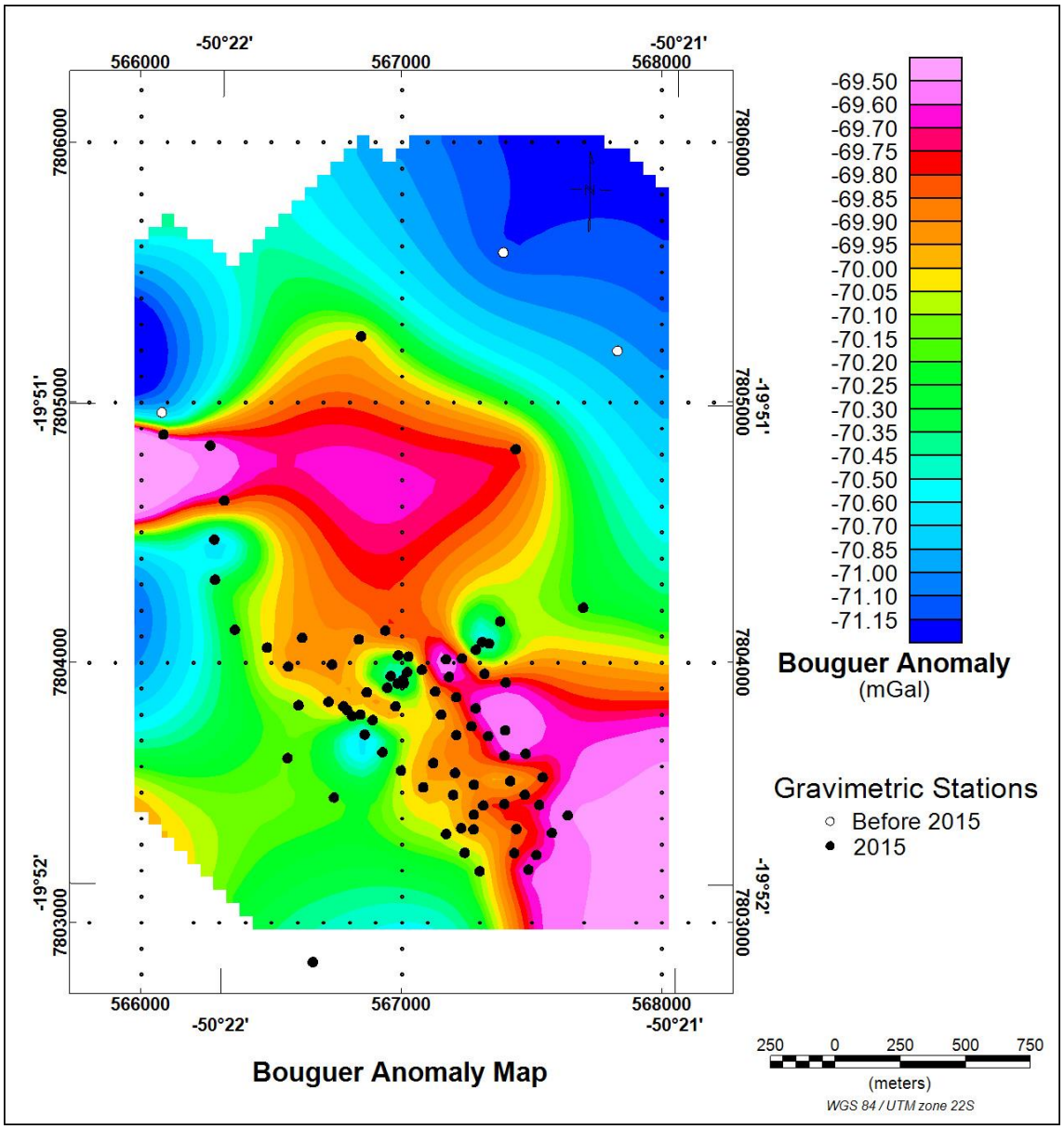

Figure 11 – Bouguer Anomaly Map using Minimum Curvature Gridding with 50m cell size. Gravimetric stations locations are in circles (black for 2015 survey and white for previous regional surveys). Bouguer anomaly map has an average grid resolution of 100 meters (the resolution is 25 meters in the area of data concentration).

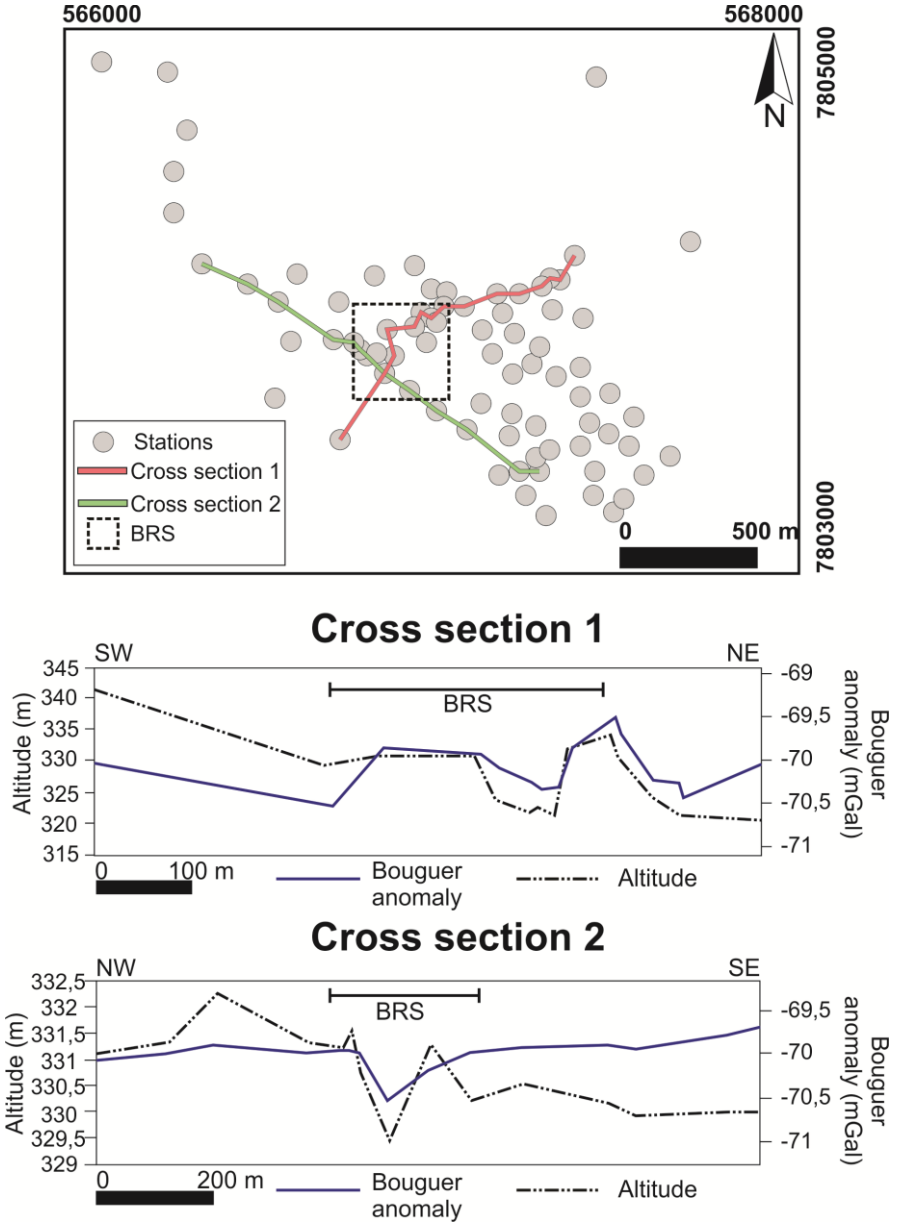
566000
568000
7805000
7803000
N
Stations
Cross section 1
Cross section 2
BRS
0
500 m
Cross section 1
SW
NE
345
340
335
330
325
320
315
Altitude (m)
BRS
-69
-69,5
-70
-70,5
-71
Bouguer anomaly (mGal)
0
100 m
Bouguer anomaly
Altitude
Cross section 2
NW
SE
332,5
332
331,5
331
330,5
330
329,5
329
Altitude (m)
BRS
-69,5
-70
-70,5
-71
Bouguer anomaly (mGal)
0
200 m
Bouguer anomaly
Altitude

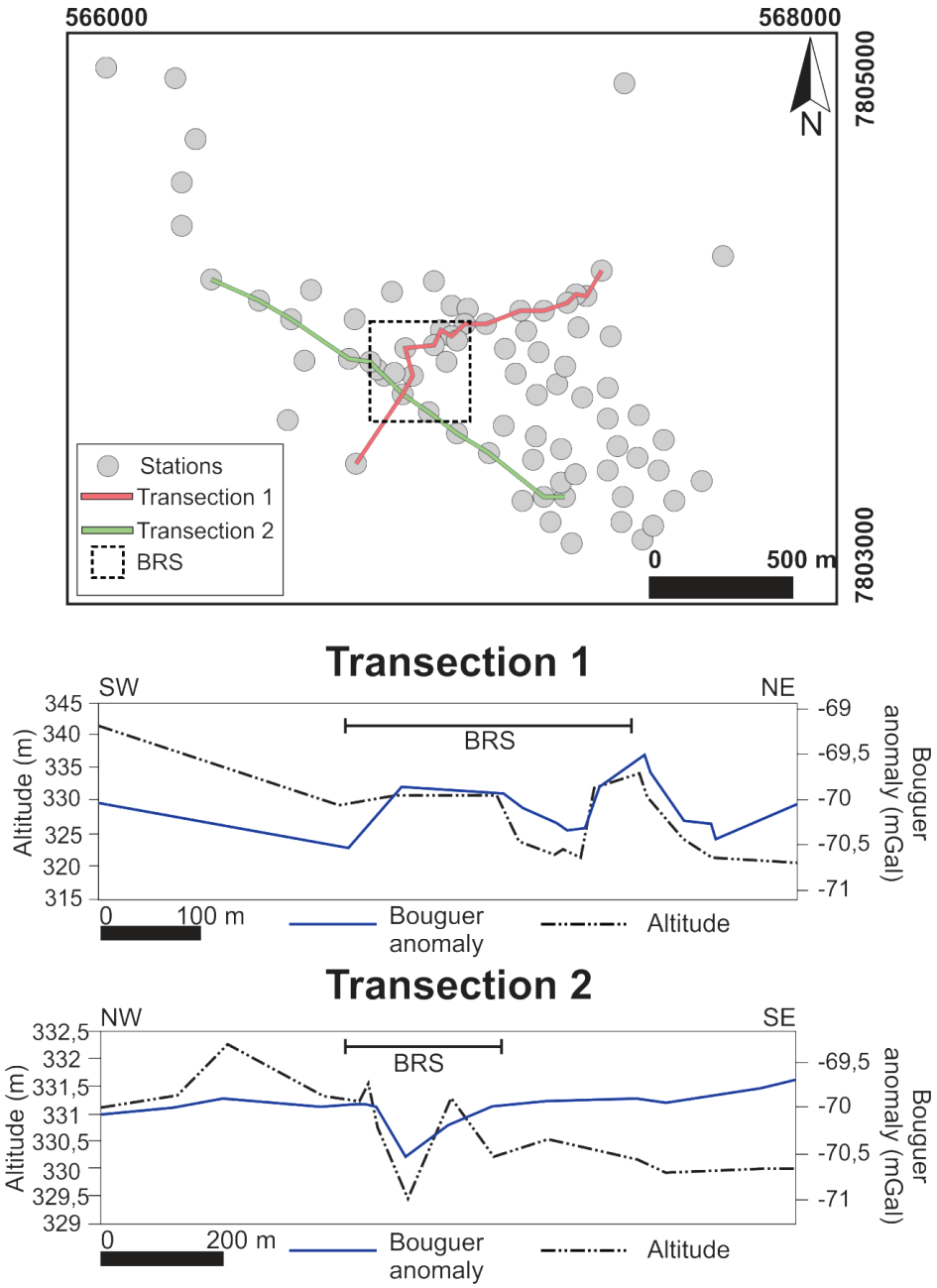

Figure 12 – Map with the gravimetric points and cross sections. The transections compare the altitude and Bouguer anomaly.

The 3D gravity forward model (Fig. 13) was done using ModelVision Software (2013) in two crossing profiles. A constant value of -70 mGal was removed as regional anomaly. The model suggests a subvertical pipe with a diameter of 70 m and an inclination of 70º. Density structure was set at 2.75g/cm3, while the background has density of 2.9 g/cm3, a typical density value for basalts. Then the structure has a density contrast of -0.15g/cm3. There is a misfit between observations and model (Fig. 13), mainly at cross section 1. This line shows small peaks of anomaly Bouguer at the border

of the structure, while the center and the outside of the structure has a low anomaly Bouguer. The tentative gravity model can explain the observations but it does not rule out any other possibility.

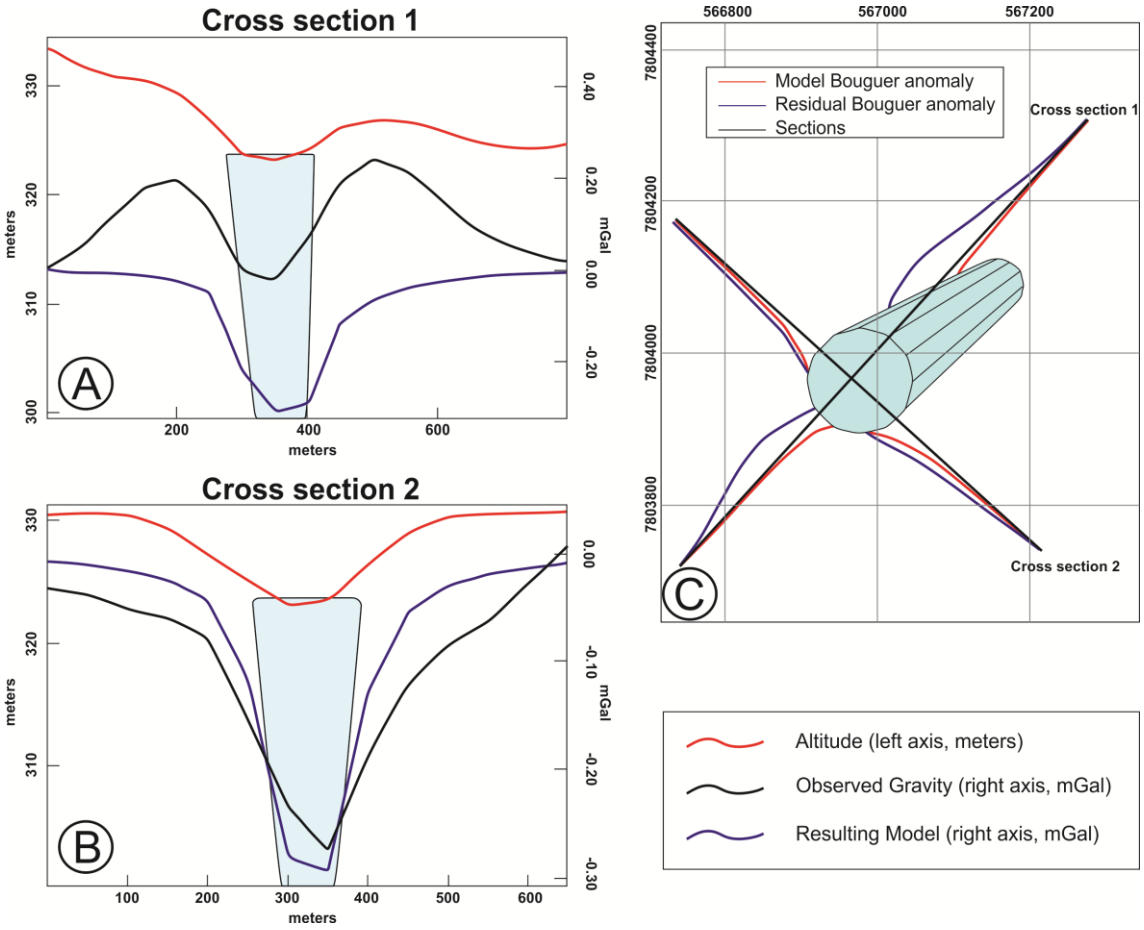

Figure 13 – 3D forward gravity model. A and B – Profiles with altitude from gravity surveys, in meters (red lines), observed gravity (black lines) and model result (blue lines), both in mGal, and pipe model. C – Profile position and modeled gravity source.

5. DISCUSSION

5.1. Significance of the basaltic ring structures

The semi-circular structure studied shows 4 types of basalts which are mineralogically similar, but differentiated by structures and textures. It is possible to identify a central vesicular-amygdaloidal flow and peripheral massive and columnar flows.

We interpret the central flow as a cooled lava lake, due to its shape and the high quantity of vesicles and amygdales oriented in degassing structures. The presence of spatter structures and the squeeze up dykes might represent the welding of lava broken

crust corroborating to an episodic explosive volcanism. According to Sumner et al. (2005) the formation of spatters is conditioned by the presence of gases in high levels, responsible for the ejection of fluid and hot pyroclastic material that, upon landing, can agglutinate and spread. Explosive volcanism can originate from a great number of factors and its combinations, such as compositional variation (magma with higher silica) or local environmental conditions that possibilitate a phreatomagmatic eruption (White et al., 2009). The presence of pahoehoe structures indicate that the lavas flowed with low velocity (Walker, 2000).

The lava flows are horizontal to sub-horizontal, with a gentle dip towards the exterior of the ring structure (see cross sections in figure 4). Due to the presence of amygdales and vesicles concentrated at the top of those flows it is possible to characterize them as lobes of pahoehoe flows of the P-type (Self et al., 1998). According to Self et al. (1998), the lobes can coalesce laterally during inflation and form flows of hundreds to thousands of meters of extension.

The basal level is represented by massive basalts with the presence of geodes and locally gas scape structures. There is no structure that records any movement during crystallization. The dykes present a ring shape with columnar joints, which are either subvertical or dipping towards the center of the structure (see cross sections in figure 4). The dykes crosscut only the basal flow. The dipping of the columns towards the center of the structure, the similar mineralogy to the basalt flows, and the arrangement of the ring dykes suggests that they could represent secondary conduits for the flows, diverging from a central conduit.

According to McKee & Straddling (1970), the BRS in Washington were formed by the collapse of the top of a thick lava flow. However, this model does not fit with the presence of an explosive event. The presence of a high volume of gases could be explained by the model of Hodges (1978) that states that a rise in the water table in contact with the flow in its fluid phase could generate phreatomagmatic explosion due to a sudden heating of the water. Although some authors suggest, however, that even in a desertic, hot and dry paleoclimate, monsoon rains would occur seasonally due to the continentality of Gondwana (Scherer & Goldberg, 2007) and that this humidity is registered in the northern portion of the basin, in the fossiliferous register of the

Botucatu Formation (Pires et al., 2011), the fetures described by Hodges (1978) are very different from those observed in Água Vermelha.

Larger ring structures related to the Etendeka side of the Paraná-Etendeka Province have been identified in Namibia (e.g. Corner, 2000). These however are usually much larger structures (ca. 100 – 200 km of diameter) associated with classic ring dykes. The ring structures of Água Vermelha are not the large scale ring structures commonly associated with large intrusive volcanic centres (e.g. Jerram & Bryan, 2015 and references therein), but moreover associated with smaller localized basaltic eruptions and lava fields.

5.2. Model for extrusion of the Serra Geral Formation in the Água Vermelha region and implications for the Paraná basin

We here present a model for the evolution of the basaltic ring structures (Fig. 14). Our model describes the volcanism of the Serra Geral Formation in the Água Vermelha region in three main steps: (1) fissure flow occurs with lava input; (2) this lava cools and crystallises cementing most of the fissures, promoting the formation of localized central conduits; and (3) the presence of dissolved gas in lava produces ring and radial fractures around the solidified lava lake. The magma uses some of the ring fissures to ascend and the following lava flows assume the ring shape of the dyke vent. This model agrees with the work of Araujo (1982).

The lava lake found in the semi-circular structure would represent one the central conduits. This lake was rich in fluids and gases, hence the high density of vesicles and amygdales and gas escape structures. These fluids were responsible for explosive episodes as attested by the presence of spatter structures.

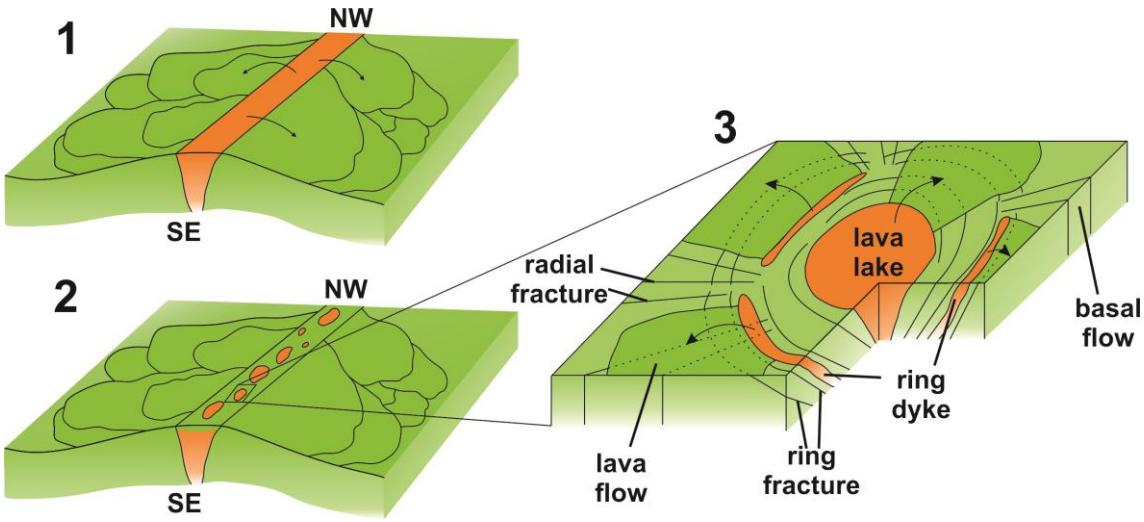

Figure 14 – A model for the evolution of fissural flows and the formation of central conduits in the Água Vermelha region: (1) fissure flow occurs with lava input; (2) this lava cools and crystallises cementing most of the fissures, promoting the formation of localized central conduits; and (3) the presence of dissolved gas in lava produces ring and radial fractures around the solidified lava lake.

The presence of gas in lava flows below already crystallized basalt was responsible for the radial and ring fracturing. The dykes used the ring fractures as novel and subsidiary conduits for the lava, which then assumed a radial shape.

The gravimetric analysis shows a positive Bouguer anomaly along the river, as seen in figure 10 through the pink and red colours. This can be explained by the higher density of the basalt among the sediments and country rocks. The local anomaly of the BRS has a negative Bouguer value compared to the surroundings. This could be due to the lower density of the material on the BRS, which can be represented by the vesicular basalt at the center of the structure or due to alteration of the minerals led by the fracture system imposed by the BRS. Also this anomaly could simply represent the topography as it overlaps the low altitude part of the cross sections, meaning that a further survey must be done to create a detailed gravimetric model and determine the main cause of the anomaly. This type of anomaly is found on Odessa's BRS, Washington, and is described as a difference of density between the material on the structure and the material surrounding them (Parks & Banami, 1971).

It is shown by our observations that the basaltic flows of the Serra Geral Formation in the Água Vermelha region were extruded through fissures, which evolved to central conduits and lava lakes. The conduits would present magmatic activity until

the cooling of the lava was enough to completely seal the top of the fissures and preserve the circular ring structures.

We can see differences between this model and the one proposed by McKee & Stradling (1970) since the sag flowout shows dykes outward-dipping because of a different evolution of the structure. The model proposed by Hodges (1978) shows an interaction between lava and water table responsible for the explosion, with tephra and presence of palagonite, but we may not assume that this happened in Serra Geral Formation since its development was during a dry climate condition and we didn't find any tephra or palagonite.

6. CONCLUSIONS

Basaltic Ring Structures of the Early Cretaceous Serra Geral Formation were identified and described in detail in the Água Vermelha region, southern Triângulo Mineiro, Paraná basin, Brazil. Although earlier works considered the BRS in Washington formed differently (McKee & Stradling, 1970; Hodges, 1978), we here present a different model for their formation, based on detailed geological mapping and petrography.

The most well-preserved of these structures presents a central lava flow characterized by a high density of amygdales and vesicles, gas scape structures such as pipes, spatter structures and pahoehoe structures. This central level is interpreted as a lava lake where explosive volcanism was common and represents the central conduit of the structure. This is superseded by at least eight different flows of massive basalt and crosscut by ring dykes, with columnar disjunctions which dips towards the center of the structure.

Thus, we interpret the Basaltic Ring Structures of the Água Vermelha Region as central conduits. Those conduits were formed when the temperature was cool enough to crystalize almost all the surface of the fissure, leaving some circular spots as lava lakes. The fluid produces radial and ring fractures around the structure and the lava escapes through some of them.

Our model has clear impacts on the interpretation of the fissural volcanism in the Paraná basin during the breakup of Gondwana and the opening of the Atlantic ocean,

the dynamics and genesis of the basaltic flows of the Serra Geral Formation, and the generation and extrusion of LMPs in general.

Artigo 2 – GEOCHEMISTRY OF BASALTIC FLOWS FROM A BASALT RING STRUCTURE OF THE SERRA GERAL FORMATION AT ÁGUA VERMELHA DAM, TRIÂNGULO MINEIRO, BRAZIL: IMPLICATIONS FOR THE MAGMATIC EVOLUTION OF THE PARANÁ-ETENDEKA PROVINCE

Fernando Estevao Rodrigues Crincoli Pacheco[1], Fabricio de Andrade Caxito[1]*, Lucia Castanheira de Moraes[2], Antonio Carlos Pedrosa-Soares[1]*, Glaucia Nascimento Queiroga[3]

[1] Universidade Federal de Minas Gerais, Programa de Pós-Graduação em Geologia, CPMTC-IGC-UFMG, Campus Pampulha, 31270-901 Belo Horizonte, MG, Brazil. (ferodrigues@live.it; boni@ufmg.br; pedrosa@pq.cnpq.br)

[2] Centro Federal de Educação Tecnológica de Minas Gerais – CEFET MG Av. Ministro Olavo Drummond, 38180-510, Araxá, MG, Brazil. (2013luciam@gmail.com)

[3] Departamento de Geologia, Escola de Minas, Universidade Federal de Ouro Preto, Morro do Cruzeiro, 35400-000, Ouro Preto, MG, Brazil. (glauciaqueiroga@yahoo.com.br)

*Fellow of the Brazilian Research Council (CNPq)

1. INTRODUCTION

The Serra Geral Formation represents a thick flow of mainly basaltic rocks (ca. 1,700 m of maximum thickness), and belong to the continental-scale Paraná-Etendeka Magmatic Province (PEMP) (Almeida, 1986). Due to its extension, its characteristics are not homogeneous. Bimodal magmatism was responsible for predominantly basaltic and subordinate rhyolitic rocks found at the province. Through studies carried throughout the province, the basalt rocks were divided into six magma-types according to their geochemical characteristics - Pitanga, Paranapanema and Urubici (HTi), Gramado, Esmeralda and Ribeira (LTi) - and the rhyolitic rocks are divided into Palmas and Chapecó types (Bellieni et al., 1984; Peate et al., 1992).

It is widely thought that the main extrusion mechanism for this rapid basaltic volcanism of the PEMP was through crustal fissures formed during the Cretaceous, due to the break-up of West Gondwana (Almeida, 1986). Dyke swarms are commonly found oriented according to tens of km-long fractures, such as the Ponta Grossa, Serra do Mar and Florianópolis (Marques & Ernesto, 2004). Those dyke swarms are commonly interpreted as feeders to the province. Except the ones of Florianópolis Swarm, whose ages are subject of some debate, the other dykes are slightly younger than the flows (e.g. Deckart et al., 1998; Renne et al., 1996). In other similar provinces, basaltic ring structures (BRS) are eventually found (e.g.: Swanson et al., 1975; Jaeger et al., 2005; Webster et al., 2006), and in the Serra Geral Formation, eleven BRS were identified on the northern area of the province and characterized as possible conduits of lava (Araújo et al. 1977; Araújo 1982; Araújo & Hasui, 1985). This descriptive term (BRS) refers to rimmed topographic depression within basaltic lava flow which appears in plain view as a circular or elliptical structure with raised rims (Burr et al., 2009).

In this paper, we present detailed petrographic, lithochemical and mineral chemistry and thermometry data from the basalts of one of those BRS situated on the Northern portion of the Serra Geral Formation, at the Triângulo Mineiro region. This study contributes to a better characterization of the BRS lava flows and to improve the understanding about the geochemical evolution of the Serra Geral Formation, since the BRS might represent a volcanic conduit and its analyses can point the magmatic source characteristics, as well as differentiation and crystallization processes that occurred on PEMP flows.

2. GEOLOGICAL CONTEXT

The development of the Paraná basin occurred during the Phanerozoic upon a crystalline and metasedimentary basement in the southeastern region of the South American platform, which was profoundly affected by tectonic, magmatic and metamorphic events during the Neoproterozoic (ca. 900 – 530 Ma) (Zalán et al., 1991). Deposition of the sedimentary-magmatic sequence that filled the Paraná basin occurred from the Upper Ordovician to the Upper Cretaceous (Milani, 2004).

The Serra Geral Formation represents more than 90% of the preserved part of the Paraná-Etendeka Magmatic Province (PEMP) and its origin is related to the breakup

of Gondwana and the opening of the South Atlantic Ocean. A thick volcanic succession which covers a great portion of southern Brazil and parts of Paraguay, Uruguay and Argentina (Marques & Ernesto, 2004) and occupies an area of approximately 9.17 x 105 km2 with about 1.7 x 10^6 km^3 of, predominantly, basaltic rocks (Frank et al., 2009), along with mafic sills and dyke swarms that crosscut the sedimentary basin, compose the PEMP (Milani et al., 2007).

The basic volcanic rocks of the Serra Geral Formation are divided into a high titanium group (HTi) and a low titanium group (LTi). Previous detailed works enabled, through element content and element ratios, the definition of six magma-types: Urubici, Pitanga, Paranapanema, Gramado, Esmeralda and Ribeira, the first three, HTi and the last three, LTi. The rhyolitic magma were separated due to the amount of incompatible elements, being the Palmas and Chapecó types depleted and enriched in those elements respectively (e.g. Bellieni et al., 1984; Mantovani et al., 1985; Piccirillo and Melfi, 1988; Peate et al., 1992).

The distribution of those magma-types is not random through the PMPE. Although the Pitanga and Paranapanema types (HTi) occur through the entire province, in volume they are preferentially located at the northern area. The LTi and rhyolitic magmas occur on the south-central part of the province (Janasi et al., 2011) (Fig. 1). The Southern Paraná Magmatic Province hosts the Urubici rocks (HTi) (Piccirillo and Melfi, 1988; Peate, 1997), although some scarce flows (Machado et al., 2007) and dykes (Seer et al., 2011; Marques et al., 2016) are found in the northern area.

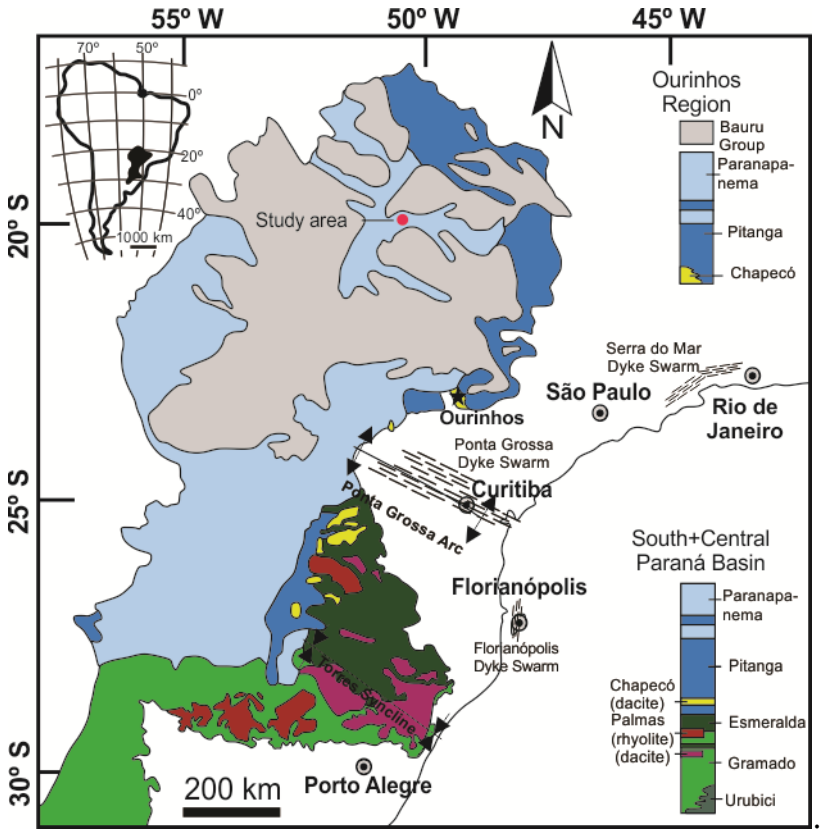

Figure 1 – Map showing the distribution of magma-types of the Serra Geral Formation throughout the Paraná Basin (adapted from Janasi et al., 2011). The study area is represented by the red dot.

2.1.Água Vermelha Region

The Água Vermelha region is located between the cities of Iturama (Minas Gerais state) and Ouroeste (São Paulo state), where a hydroelectric dam was constructed over the Grande riverbed. The geological studies in the region date from the time of construction of the dam, (e.g. Araújo et al., 1977; Araújo, 1982; Araújo & Hasui. 1985). Basaltic rocks of the Serra Geral Formation in the area occur as both dykes and lava flows. The flows are distributed in conspicuous semi-circular structures, while the dykes are disposed in ring structures (Araújo, 1982). Also, in the center of one BRS a lava lake structure was described, which is surrounded by lava flows and a ring dyke (Pacheco et al., 2017).

Three types of mafic rocks characterize the lava flows described in the region: basaltic breccias, vesicle-amygdaloidal basalts and massive basalts. The basaltic breccias are restricted and divided into volcanic and pyroclastic types. The semi-circular structures are expressed in the region as depressions and numbered from 1 to 11 in the Figure 2. They are filled by vesicular-amygdaloidal basalts, with pahoehoe structures,

and show a sharp contact with neighboring lava flows or ring dyke. Ring fractures are common (Araújo & Hasui, 1985).

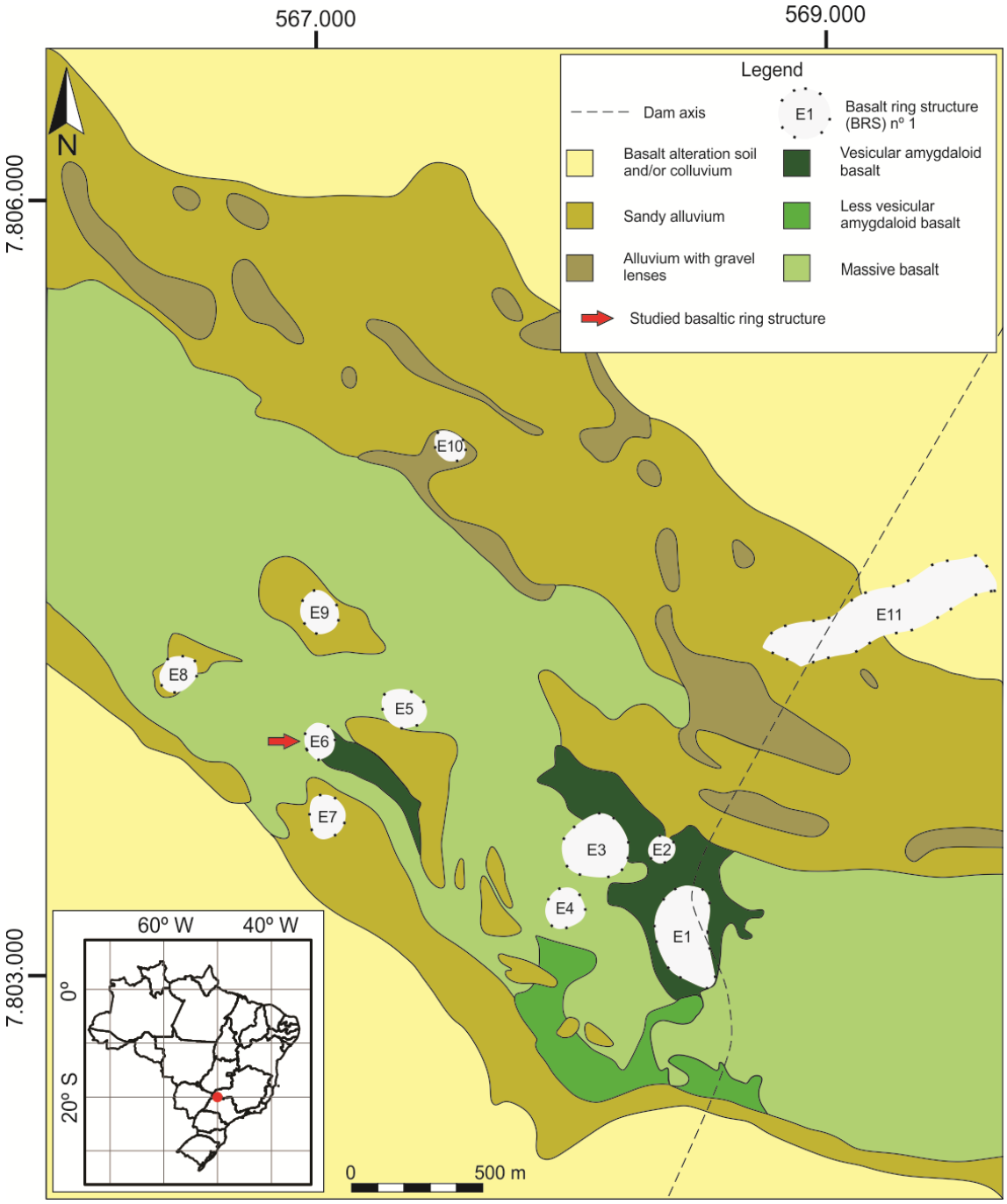

Figure 2 – Geological map of the Água Vermelha region. Adapted from Araújo (1982). Coordinates are in UTM, WGS 84 Datum.

3. MATERIALS AND METHODS

To characterize each flow of the BRS, a petrographic study was made with samples of each level through 30 thin sections to detail the texture and mineralogical components and 5 polished sections were made for mineral chemistry analyses. The

samples used for chemical analyses (both mineral chemistry and lithochemistry) are represented on the stratigraphic sections (Fig. 4).

The microanalysis of plagioclase, pyroxene and titanomagnetite were performed with an electron microprobe JEOL JXA-8900RL at the Microscopy and Microanalysis Laboratory of the Centro de Desenvolvimento da Tecnologia Nuclear CDTN/UFMG. The electron beam was set at 15 kV, 20 nA, 2-5 μm and the common matrix ZAF corrections were applied. Counting times on the peaks/background were 10/5 s for all elements (Si, Na, Mg, Mn, K, Al, Fe, Ca, Ti), except for Cr and P (20/10 s). Analytical errors are within 0.12% and 1.23%. Plagioclase and clinopyroxene were analyzed along granular spots and analyses from core and rims. Table 1 summarizes the main features of the analysis, as the analyzed elements and standards. The mineral formulas were calculated based on 6 oxygens for pyroxene and 8 for plagioclase crystals. The total iron content obtained by the microprobe was considered as FeO. The pyroxene thermometry was calculated based on Lindsley (1983) P = 1 atm. The binary and ternary diagrams used to characterize the main minerals were obtained by Excel and GCDKit 2.3.

Table 1 – Overview of the major element set-up for clinopyroxene, plagioclase and titanomagnetite analysis. TAP - Thallium acid phthalate crystal; PET - Pentaerythritol crystal; LIF – Lithium fluoride crystal.

Elements	Energetic Line	Crystal	Standard
Si	Kα	TAP	Quartz
Na	Kα	TAP	Anortoclase
Cr	Kα	LIF	Cr_2O_3
P	Kα	PET	Apatite
Mg	Kα	TAP	MgO
Mn	Kα	LIF	Mn-Hortonolite
K	Kα	PET	Anortoclase
Al	Kα	TAP	Corindon
Fe	Kα	LIF	Magnetite
Ca	Kα	PET	Apatite
Ti	Kα	PET	Rutile

The whole rock chemical analyses preparation consisted of the crushing and pulverization of ca. 300g of homogeneous and unweathered sample on a tungsten carbide shatterbox at the Sample Preparation Laboratory of the CPMTC-IGC-UFMG. The sample analyses followed the ICP (Induced Coupled Plasma) routine at SGS Geosol Laboratories. The major elements were analyzed by ICP-OES (Induced Coupled Plasma – Optical Emission Spectroscopy) and the minor and trace elements by ICP-MS

(Induced Coupled Plasma – Mass Spectrometry). The accuracy and precision are better than 10% and the confidence level is 95%.

The major elements diagrams and the CIPW norm were made after normalization on water-free basis (Gill, 2014). The CIPW norm of the standard mineral components, from the whole-rock analyses, was based on Johannsen (1931). Since the whole-rock chemical analyses considered only Fe_2O_3, the estimation of FeO and Fe_2O_3 was based on Gill (2014), with $\Sigma Fe_2O_3 = (1.11 \times FeO) + Fe_2O_3$.

4. PETROGRAPHY

The rocks of the BRS were divided in flows due to the easily identifiable top and basal sharp contact of each flow and are represented in the geological map (Fig. 3, Pacheco et al, 2017) and stratigraphic columns (Fig. 4, Pacheco et al, 2017). Nomenclature of each flow follows the numeric order of superposition and lateral continuity. In case where it was not possible to determine the lateral correlation of each flow a new sequence was adopted, resulting in two different numberings: 0 to 8 and 1A to 3A; both occur above the basal flow. Dykes crosscut the basalts and the central flow is composed of vesicle-amygdaloidal basalt which is very distinct from the other flows.

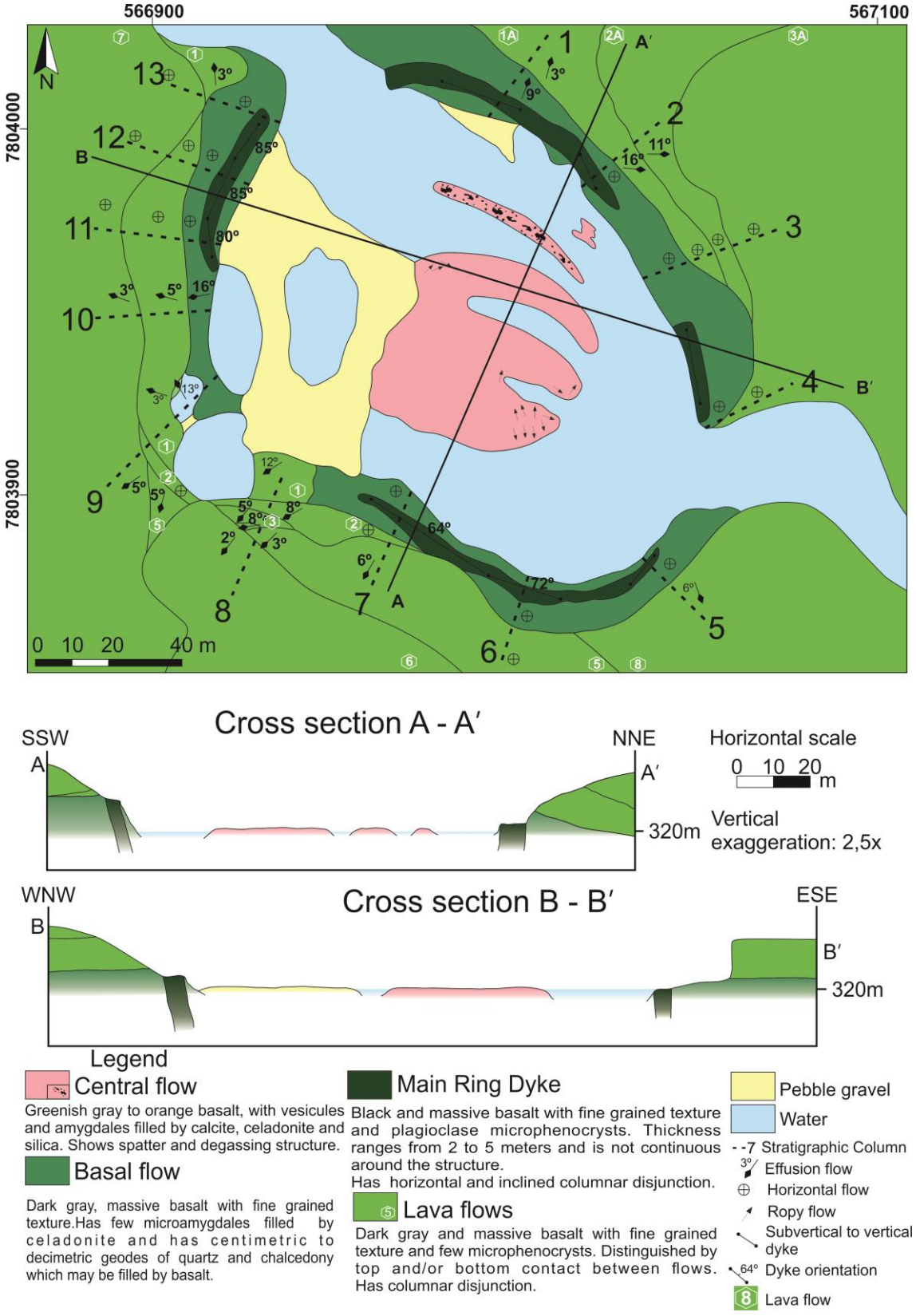

Figure 3 – Geological map of Basalt Ring Structure E6 in Água Vermelha region, MG/SP, Brazil, showing the different basalt flows, structures and location of the studied stratigraphic sections (Pacheco et al., 2017).

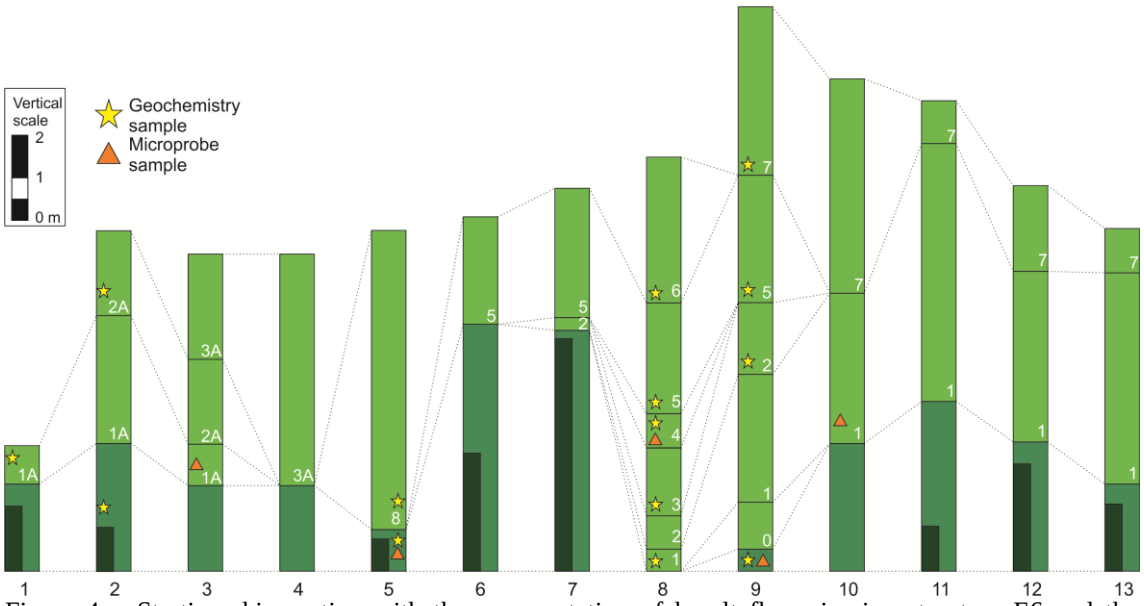

Figure 4 – Stratigraphic section with the representation of basalt flows in ring structure E6 and the location of the lithochemical and microprobe samples analyzed. The location of each column is represented in the geological map of Fig. 3 by a dashed line. Column number 1 is on the Northern part of the area and the following columns were made clockwise direction until number 13. Adapted from Pacheco et al. (2017).

4.1.Central flow

The central flow is composed of grayish vesicle-amygdaloidal basalt, which is orange when weathered (Fig. 5A). In thin sections, the sample has a predominant intergranular texture with a smaller amount of glass between the crystals. The plagioclase laths are euhedral to subhedral with a size of 0.2-0.8 mm showing Carlsbad twinning and the clinopyroxene crystals are granular and smaller than 0.5 mm. The amygdala is filled with tabular zeolite crystals (0.1-0.5mm) and calcite matrix (Fig. 5B).

It is possible to identify spatter structures of variable size, milimetric to centimetric, reaching up to 15 cm long (Fig. 5C). The spatter structure has a vitreous matrix and shows larger plagioclase laths (0.5-1.5 mm) than the intergranular vesicle-amygdaloidal matrix (0.2-0.8 mm). The plagioclase shows “swallow-tail” endings (Fig. 5D).

The degassing pipes structures reach 15 cm of diameter (Fig. 5E). In thin sections, they show a vitreous matrix with plagioclase laths smaller than 1 mm, granular clinopyroxene crystals smaller than 0.4 mm and amygdala filled with zeolite (Fig. 5F).

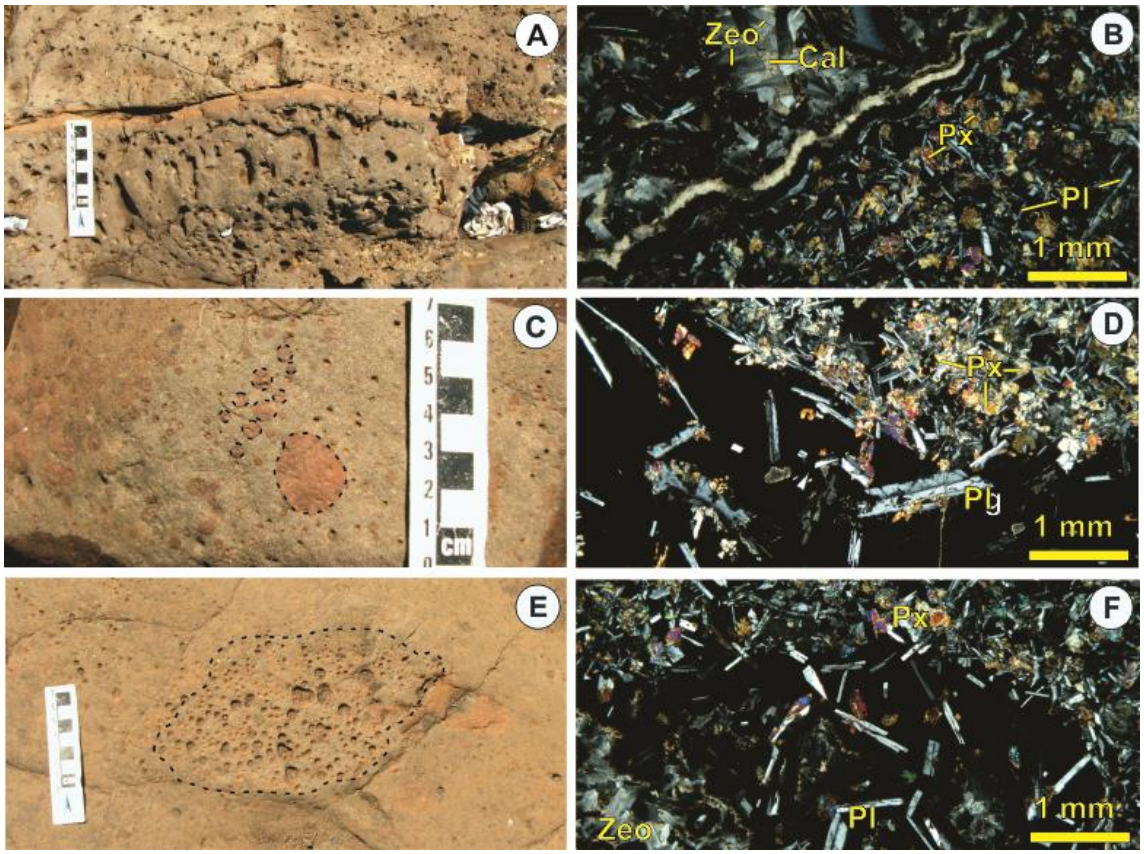

Figure 5 – A – Central flow vesicle-amygdaloidal basalt. B – Photomicrography of the central lava flow, with intergranular texture and amygdala filled by zeolite and calcite. C – Spatter structure. D – Photomicrography of spatter structure well-marked by glass and laths. E – Degassing pipe structure. F – Photomicrography of the degassing pipe structure with plagioclase and clinopyroxene laths wrapped by glass and amygdales filled by zeolites. Pl = plagioclase, Px = pyroxene, Zeo = zeolite, Cal = calcite. All photomicrographs under crossed polarizers.

4.2.Basal flow

The basal flow is composed of homogeneous and massive dark grey basalt, with fine-grained plagioclase and pyroxene. It may rarely show some microamygdales (1 – 2 mm) filled by celadonite, and towards the top of the flow centimetric to decametric quartz geodes occur, reaching up to 60 cm in diameter (Fig. 6A). In thin section, it has a predominantly intergranular texture with a smaller amount of glass between the crystals. The plagioclase laths are euhedral to subhedral, smaller than 0.3 mm, showing Carlsbad twinning, and the clinopyroxene crystals are granular and smaller than 0.1 mm. Microphenocrysts of plagioclase forming glomeroporphyritic aggregates are occasionally observed, with 0.5-1.0 mm in size, showing Carlsbad twinning and concentric zoning (Fig. 6B). Iddingsite can be found as an olivine pseudomorph and

opaque minerals (oxides) occur, with cubic, prismatic and skeletal habit and smaller than 0.1 mm (Fig. 6C and 6D).

4.3.Main ring dyke

It is composed of black basalt with a thickness from 2 to 5 meters, showing inclined to horizontal columnar disjunctions and it is discontinuous throughout the structure (Fig 6E). In thin section, it has a predominantly intergranular texture with a smaller amount of glass between the crystals. The plagioclase laths are euhedral to subhedral, with size of 0.1 to 0.8 mm, showing Carlsbad twinning and "swallow-tail" endings. The pyroxene crystals are granular and smaller than 0.1 mm. Microamygdales (smaller than 1 mm) are filled with clay mineral (Fig. 6F).

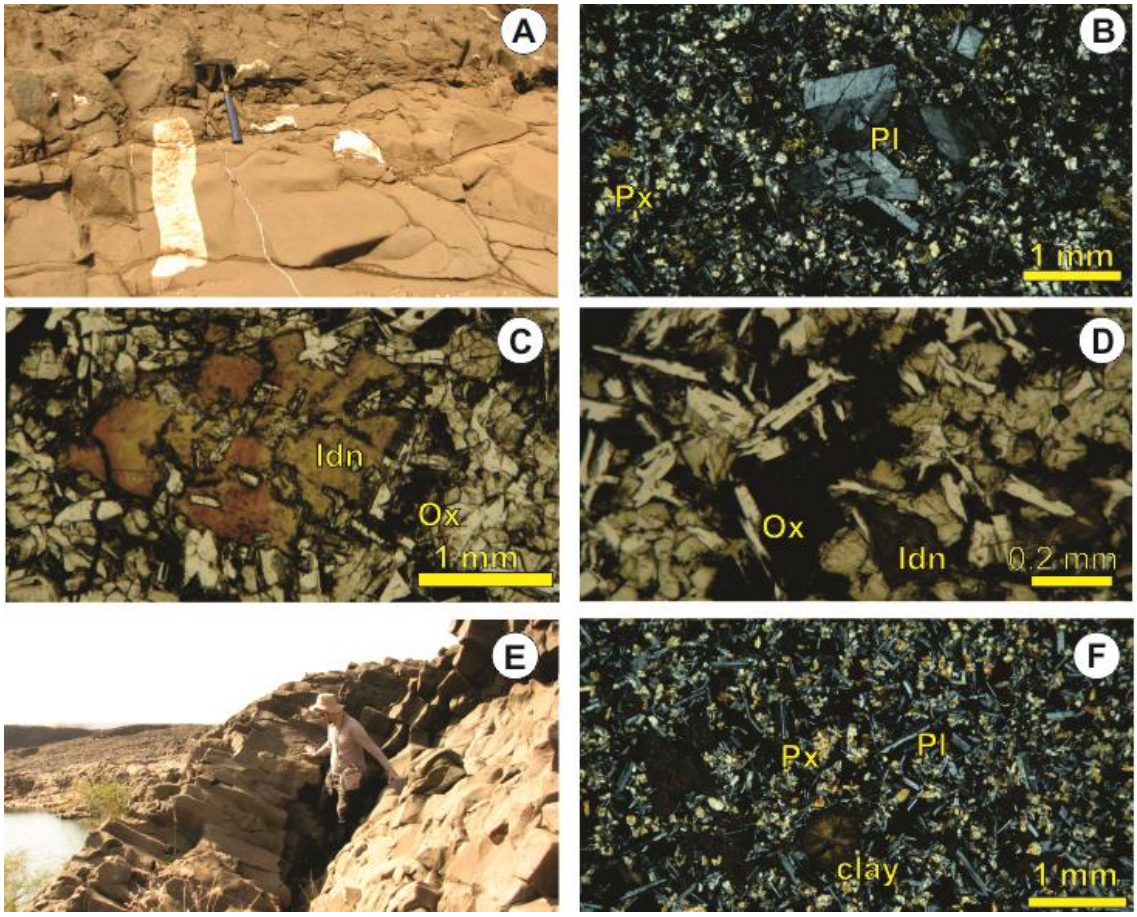

Figure 6 – A – Basal flow general aspect, with quartz geode. Photomicrographs of the basal flow basalt, showing glomeroporphyritic aggregate of plagioclase (B), iddingsite and oxides (C and D). E – Main ring dyke basalt with inclined columnar disjunction. F – Main ring dyke photomicrography with plagioclase and pyroxene laths, glass and microamygdales filled with clay. Pl = plagioclase, Px = pyroxene, Idn =

iddingsita, Ox = oxide. Photomicrographs B and F under crossed polarizers and C and D under parallel polarizers. A and E from Pacheco et al. (2017).

4.4. Lava flows

The lava flows are composed of massive dark grey basalts, with fine phaneritic to aphanitic texture, with rare microphenocrysts. They are separated by sharp top and base contacts and show columnar disjunctions (Fig. 7A).

In thin section, the rock has a subophitic texture with a small amount of glass between the crystals. The matrix has plagioclase laths smaller than 0.5 mm, with Carlsbad twinning and "swallow-tail" endings and granular pyroxene smaller than 0.2 mm. The rock presents microphenocrysts of plagioclase (1-2 mm) which can show Carlsbad twinning, concentric and hourglass zoning (Fig. 7B, 7C and 7D). Microphenocrysts of plagioclase and pyroxene forming glomeroporphyritic aggregates are occasionally observed, with 0.5-1.2 mm in size (Fig. 7E). Iddingsite can be found as an olivine pseudomorph and opaque minerals (oxide) occur, with cubic and prismatic habits and smaller than 0.1 mm.

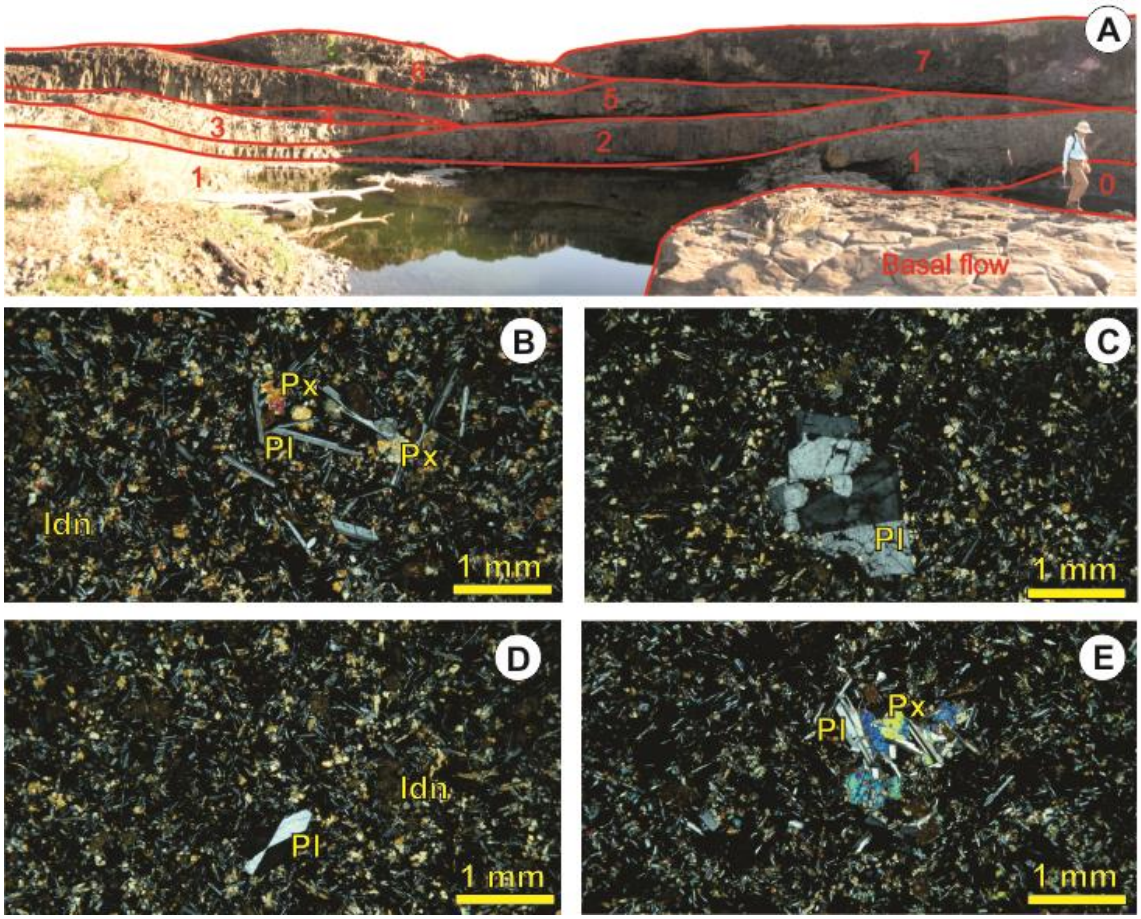

Figure 7 – A – Lava flows mapped in the southwestern edge of the mapped ring structure. UTM coordinates: 7803986 N/567020 E/Zone 22K/ facing southwest (Pacheco et al., 2017). B-E – Photomicrographs of the lava flow, showing phenocrysts of plagioclase and pyroxene (B), plagioclase

with concentric (C) and hourglass zoning (D), and glomeroporphyritic aggregates of plagioclase and pyroxene. Pl = plagioclase, Px = pyroxene, Idn = iddingsite, Ox = oxide. All photomicrographs under crossed polarizers.

5. LITHOCHEMISTRY

The major, minor and trace elements analysis and the CIPW norm of 14 samples are presented on Table 2. Those data were used to elaborate diagrams which assisted in the lithochemistry interpretation of the studied rocks, being 11 samples from the lava flow (LF) and 3 samples from the basal flow (BF).

The samples did not suffer any significant post-magmatic alteration as indicated by their LOI contents (< 1%) and are classified as basic rocks (SiO_2 = 48.02 – 50.65 %). The content of alkali elements ($Na_2O + K_2O$ = 3.06 – 3.28%), Al_2O_3 (12.62 – 13.62 %), Fe_2O_3T (13.83 – 15.04 %), MgO (5.56 – 6.28 %) and CaO (9.76 – 10.58%) are within the range for basaltic rocks. Those values were calculated on anidre basis.

All samples plot on the subalkaline basalts field on the TAS (Total Alkalis/Silica) diagram (Le Maitre, 2002), within the field of tholeiitic basalts (MacDonald & Katsura, 1964) (Fig. 8A). The basalts of Água Vermelha belong to the high titanium group (1.96% < TiO_2 < 2.14%) according to the magma-type classification of Peate et al. (1992). The Sr vs. TiO_2 and Ti/Y vs. Sr diagrams (Peate et al., 1992; Machado et al., 2007) show that all of the samples plot within the Paranapanema field (Fig. 8B and 8C). It is possible to identify some crustal contamination based on the $(Th/Nb)_{PM}$ vs. $(Sm/Yb)_{PM}$ ratios (Wang et al. 2007). The higher $(Th/Nb)_{PM}$ ratios belong to samples from the lava flow (Fig. 8D).

Table 2 – Whole-rock analyses of basalts from the ring structure E6 and CIPW norm data. LF – Lava Flow; BF = Basal Flow; An = anorthite; Ab = albite; Or = orthoclase; Di = diopside; Hd = hedenbergite; Ens = enstatita; Fs = ferrossilite; Il = ilmenita; Mag = magnetite; Fo = forsterite; Fy = fayalite.

Sample	**001**	**002**	**003b**	**004**	**005**	**006**	**007**
Level	**LF 1**	**LF 3**	**LF 4**	**LF 5**	**LF 6**	**BF**	**LF 2**
North	7,803,907	7,803,933	7,803,933	7,803,884	7,803,881	7,803,986	7,803,986
East	566,934	566,906	566,906	566,898	566,933	567,020	567,020
Major elements (wt %)							
SiO_2	50.35	48.49	49.25	48.79	49.53	48.58	49.87
TiO_2	2.01	1.99	1.97	2.01	2.13	2.02	2.02
Al_2O_3	13.46	13.08	13.12	13.41	13.37	13.22	13.46
Fe_2O_3(t)	14.23	14.13	13.99	14.08	14.96	14.55	14.28
MnO	0.21	0.20	0.20	0.20	0.20	0.21	0.22
MgO	6.03	5.86	5.87	5.96	6.01	6.22	6.00
CaO	10.49	10.13	10.29	10.2	10.27	10.33	10.51
Na_2O	2.67	2.68	2.66	2.67	2.78	2.48	2.68
K_2O	0.57	0.48	0.52	0.49	0.48	0.55	0.54
P_2O_5	0.21	0.21	0.22	0.22	0.22	0.21	0.22
Cr_2O_3	0.01	0.01	0.01	0.01	0.01	0.01	0.01
LOI	0.60	0.55	0.68	0.74	0.53	0.94	0.64
Total	100.86	97.81	98.79	98.79	100.5	99.34	100.46
Minor and trace elements (ppm)							
Zn	90	97	90	87	93	90	90
Cu	234	237	233	232	238	226	229
Ni	69	72	68	64	64	66	67
Ba	286	263	265	265	266	283	258
Cs	0.36	0.35	0.24	0.17	0.3	0.45	0.22
Ga	20.5	20.7	20.5	20.7	20.9	20.1	20.4
Hf	4.73	9.13	12.5	3.94	4.04	3.74	3.9
Nb	20.34	17.25	21.18	12.1	12.91	16.31	11.93
Rb	20.3	16.3	14.8	14.7	15.5	15.3	17.1
Sn	3.1	5.1	8.2	<0.3	2.7	0.5	0.5
Sr	312	299	306	303	300	309	308
Th	4.5	9.7	14.7	2.7	2.9	3.4	2.6
U	0.61	1.03	2	0.56	0.57	1.05	0.53
V	426	415	427	413	412	400	412
Zr	128	194	230	114	128	114	126
Y	29.74	30.02	31.45	29.16	29.93	28.17	28.82
La	23.6	21.7	22.2	25.7	20.9	20.1	22
Ce	43.9	43.5	43.5	43.8	43.1	41.3	42.4
Pr	5.68	5.57	5.62	5.52	5.59	5.35	5.48
Nd	22.5	22.7	23	22.7	22.8	21.9	22.2
Sm	5.5	5.6	5.6	5.5	5.6	5.4	5.3
Eu	1.71	1.71	1.67	1.69	1.72	1.62	1.7
Gd	5.73	6.06	5.91	5.82	5.81	5.62	5.63
Tb	0.94	0.96	1	0.9	0.92	0.88	0.89
Dy	5.88	5.96	6.4	5.73	5.77	5.59	5.69
Ho	1.16	1.21	1.35	1.15	1.15	1.12	1.12
Er	3.28	3.47	4.06	3.12	3.26	3.05	3.12
Tm	0.46	0.52	0.63	0.46	0.46	0.46	0.45
Yb	3.1	3.5	4.4	3	3	3	3
Lu	0.44	0.5	0.62	0.43	0.43	0.43	0.42
CIPW Norm (%)							
An	23.01	22.87	22.76	23.62	22.60	23.70	23.15
Ab	22.54	23.32	22.95	23.05	23.54	21.33	22.72
Or	3.36	2.92	3.13	2.95	2.84	3.30	3.20
Di	11.81	11.64	11.90	11.44	11.31	11.63	11.84
Hd	12.25	12.35	12.48	11.86	12.35	12.00	12.38
Ens	8.27	7.09	7.94	7.21	6.55	7.37	7.48
Fs	9.84	8.62	9.54	8.58	8.21	8.72	8.98
Il	3.81	3.89	3.81	3.89	4.05	3.90	3.84
Mag	2.68	2.75	2.70	2.72	2.83	2.80	2.71
Fo	0.87	1.77	1.01	1.84	2.23	2.10	1.40
Fy	1.14	2.37	1.34	2.41	3.08	2.73	1.85
Total	99.58	99.58	99.57	99.57	99.58	99.57	99.56

Sample	**008**	**010**	**015**	**016**	**023**	**024**	**026**
Level	**LF 5-S**	**LF 7**	**LF 1A**	**LF 2A**	**BF-NO**	**LF 8**	**BF-N**
North	7,803,888	7,804,008	7,804,013	7,803,894	7,803,905	7,803,881	7,804,032
East	566,945	566,915	566,926	566,958	566,968	567,050	566,976
				Major elements (wt %)			
SiO_2	49.58	48.15	47.63	47.29	47.64	48.1	48.66
TiO_2	2.05	1.96	1.98	1.95	1.94	1.97	1.97
Al_2O_3	13.54	13.09	13.20	12.67	12.52	13.05	13.19
Fe_2O_3(t)	14.45	13.9	14.03	13.94	14.06	13.74	14.06
MnO	0.21	0.20	0.21	0.19	0.18	0.20	0.20
MgO	6.10	5.87	5.78	5.55	5.52	5.87	5.95
CaO	10.32	9.97	9.91	9.69	9.83	10.08	10.16
Na_2O	2.73	2.54	2.68	2.56	2.61	2.61	2.66
K_2O	0.53	0.59	0.50	0.55	0.52	0.50	0.53
P_2O_5	0.21	0.22	0.21	0.21	0.21	0.21	0.22
Cr_2O_3	0.01	0.01	0.01	0.01	0.01	0.01	0.01
LOI	0.56	0.55	0.49	0.64	0.75	0.66	0.64
Total	100.3	97.05	96.63	95.25	95.79	96.99	98.24
				Minor and trace elements (ppm)			
Zn	89	90	82	83	82	86	87
Cu	237	229	224	226	220	230	226
Ni	68	64	64	63	62	63	66
Ba	273	295	270	261	310	286	269
Cs	0.2	0.33	0.29	0.39	0.31	0.17	0.36
Ga	20.8	20.3	20	19.7	19.9	20.5	20
Hf	3.94	3.85	5.51	3.77	4.29	3.97	3.78
Nb	-	12.16	17.38	11.78	15.15	12.2	12.1
Rb	15.2	17.3	15.1	21.1	19.3	14	19.6
Sn	2.3	2.3	3.3	2.3	0.9	<0.3	0.8
Sr	307	298	309	289	296	304	303
Th	2.5	2.8	5.6	2.6	3.3	2.8	3
U	0.68	0.59	0.95	0.51	0.66	0.55	0.57
V	436	414	411	397	411	404	421
Zr	118	113	132	112	115	114	116
Y	29.31	28.65	28.53	28.14	28.49	28.93	29.23
La	23.1	20.2	22.2	19.3	21.4	20.2	23.1
Ce	43.3	41.7	41.4	40.7	41.5	41	42.2
Pr	5.6	5.43	5.3	5.29	5.42	5.37	5.51
Nd	22.7	22.5	21.7	21.8	22.1	21.7	22.3
Sm	5.5	5.3	5.3	5.4	5.3	5.1	5.3
Eu	1.72	1.66	1.6	1.65	1.66	1.61	1.59
Gd	5.75	5.68	5.59	5.52	5.58	5.52	5.5
Tb	0.9	0.89	0.89	0.86	0.88	0.89	0.89
Dy	5.72	5.61	5.58	5.42	5.47	5.48	5.5
Ho	1.13	1.12	1.11	1.09	1.11	1.12	1.08
Er	3.23	3.16	3.08	3.03	3.09	3.13	3.12
Tm	0.45	0.45	0.46	0.42	0.44	0.44	0.44
Yb	3	2.9	3	2.9	2.9	2.9	2.9
Lu	0.44	0.44	0.44	0.41	0.44	0.42	0.42
				CIPW Norm (%)			
An	23.19	23.39	23.42	22.68	22.00	23.27	23.50
Ab	23.17	22.27	23.59	22.9	23.24	22.93	22.74
Or	3.14	3.61	3.07	3.44	3.23	3.07	3.32
Di	11.48	11.36	11.17	11.14	11.52	11.76	11.70
Hd	11.95	11.83	11.92	12.32	12.95	12.07	11.75
Ens	6.87	7.81	6.21	7.68	7.56	7.49	7.85
Fs	8.20	9.33	7.60	9.75	9.75	8.81	9.04
Il	3.90	3.86	3.91	3.91	3.88	3.88	3.77
Mag	2.74	2.72	2.76	2.79	2.80	2.70	2.66
Fo	2.13	1.45	2.51	1.24	1.10	1.57	1.44
Fy	2.80	1.91	3.39	1.73	1.56	2.03	1.82
Total	99.58	99.56	99.56	99.58	99.59	99.57	99.58

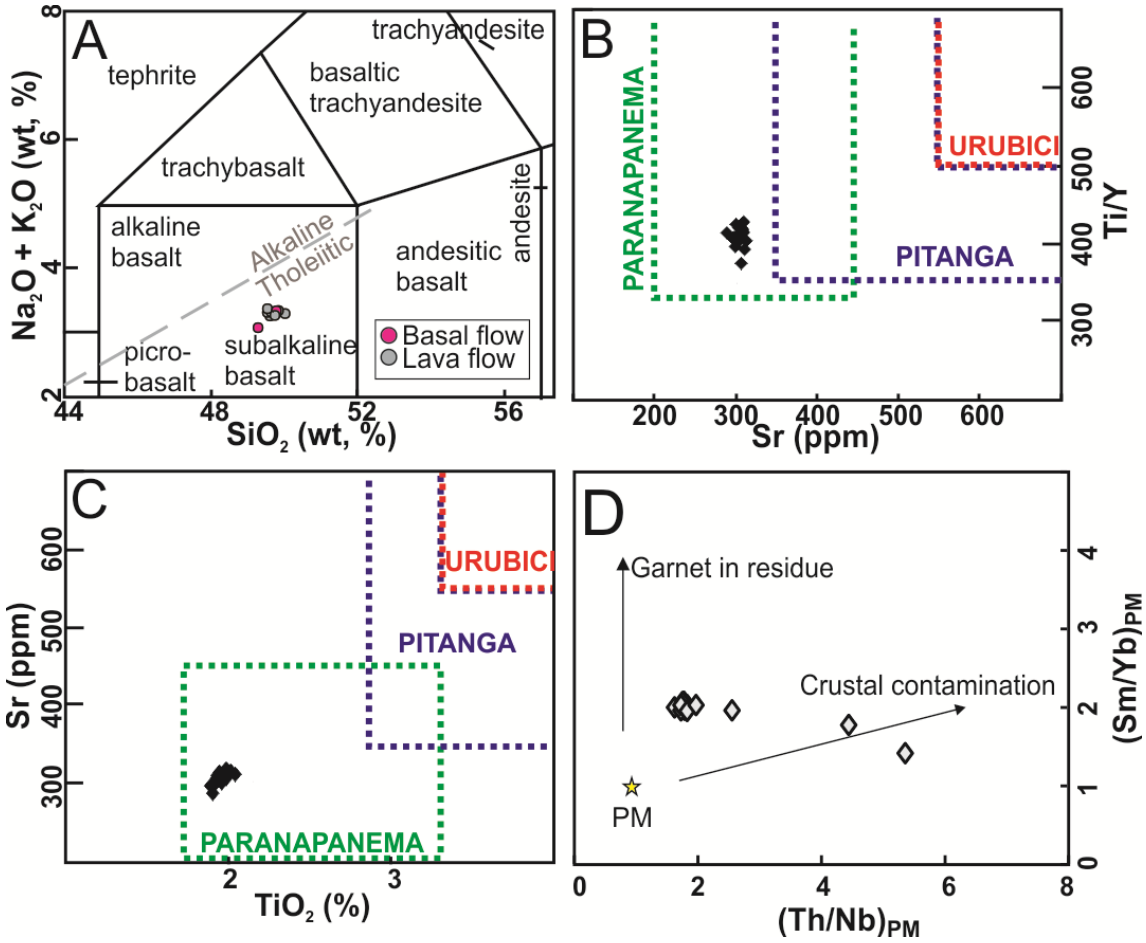

Figure 8 – A – TAS diagram (Le Maitre, 2002) with the line that divides the alkaline and tholeiitic rocks fields (MacDonald & Katsura, 1964). B and C – Diagrams for discrimination of high titanium magma-types of the Paraná-Etendeka Province (Peate et al., 1992; Machado et al., 2007). D – $(Th/Nb)_{PM}$ vs. $(Sm/Yb)_{PM}$ diagram for crustal contamination (Wang et al., 2007).

The covariation of major and trace incompatible elements can be seen through bivariate diagrams using MgO as an index for differentiation. The determination coefficientsof major elements (R^2, adjustment measure of a generalized linear statistical model) show moderate (31%, FeO_T; 49% TiO_2, 51% SiO_2) and high (72% to Al) values and when analyzing trace incompatible elements, they show low (<20%, Rb, Ba, La, U, Th) and moderate (54%, Sr) values (Fig. 9). This could be due to variable crustal contamination processes or magma mixing which would mask the magmatic differentiation process during its evolution, however the MgO variation is very small to infer about those processes.

Both LILE (Large-Ion Lithophile Elements) and HFSE (High Field Strength Elements) are enriched when normalized to the primitive mantle (Fig. 10A). Among the LILE there is a negative Sr anomaly common to all samples. Among the HFSE there is

a negative Nb, positive Zr (sample 002) and positive Th (samples 001, 002, 003b and 015) anomalies. Other elements show very similar pattern. The $(Rb/Ba)_{PM}$ ratio have a strong negative anomaly (0.54–0.8), pointing that the crustal contamination did not take place on the lava ascension (Marques et al., 2007).

The REE (Rare Earth Elements) when normalized to the chondrite (Sun & Mc Donough, 1989), show an enrichment on the total elemental concentration, higher on the LREE and lower on the HREE ($(La/Yb)_N$ = 4.34-6.14 and $(La/Sm)_N$ = 2.31-3.02) (Fig. 10B), and a negative Eu anomaly (Eu/Eu* = 0.85-0.94). When those analyses are compared to Pinto & Hartmann (2011) data for the Paranapanema type (gray field on Fig. 10B), the patterns are very similar. This enrichment could be enabled by the fractional crystallization of the magma.

The HFSE and REE arrangement (Thompson et al., 1984) normalized to the MORB (Sun & McDonough, 1989) can demonstrate features of the original magma (Pearce, 2008). The significant negative Nb anomaly (Fig. 10C) is a characteristic chemical signature for some continental flood basalt (eg. Arndt & Christensen, 1992; Pik et al., 1999), reflecting the source composition and melt conditions (Turner & Hawkesworth, 1995). In other CFB provinces, some authors interpret the subcontinental lithospheric mantle (SCLM) fusion due to a mantle plume and/or extension and decompression of the lithosphere (Reichow et al., 2005) that has been previously metassomatized during subduction process (Wang et al., 2008). The PEMP model for melt generation suggests the partial fusion of peridodite on the SCLM, due to previous processes in the mantle sources, such as the negative Nb anomaly (Turner et al., 1996).

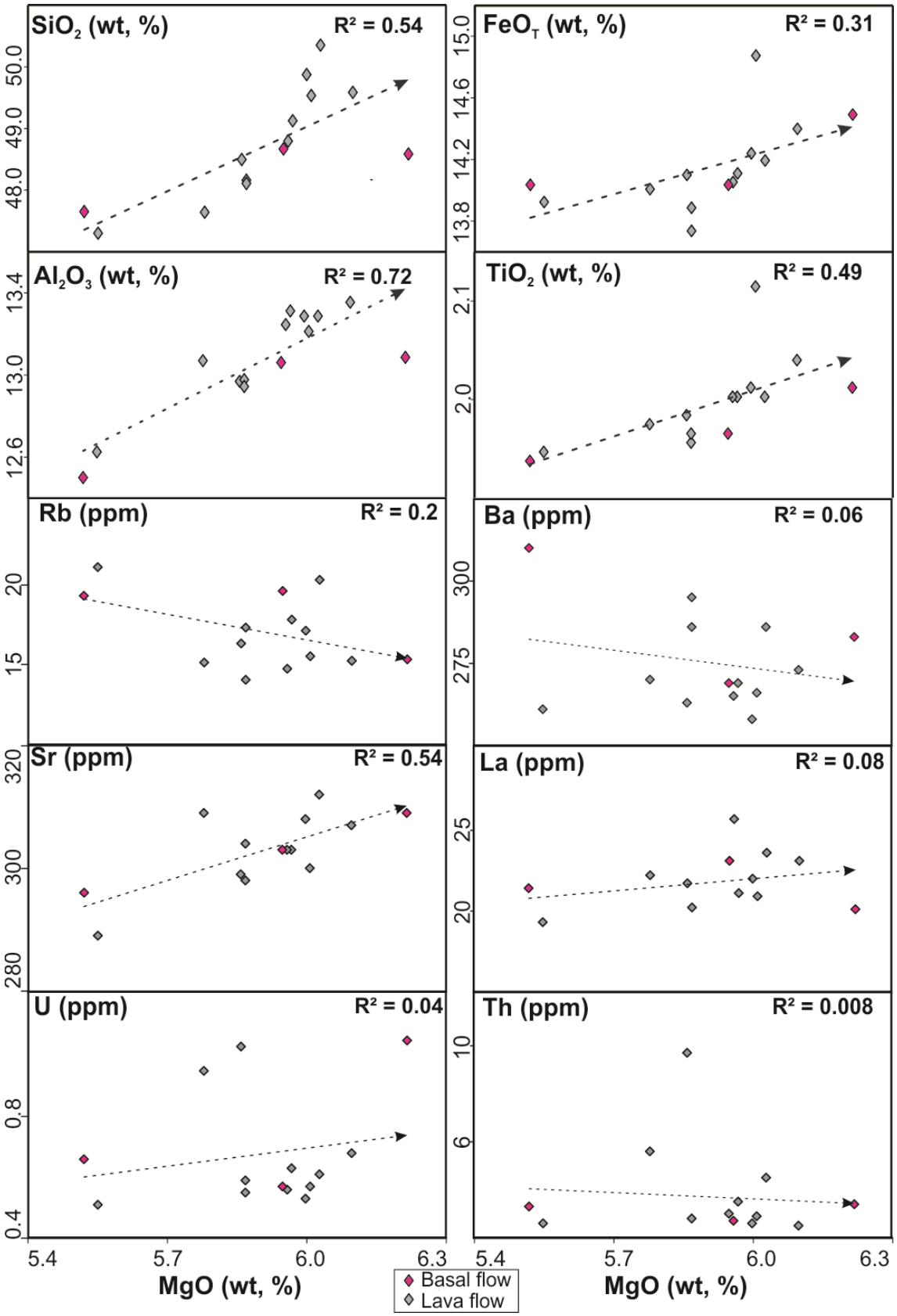

Figure 9 – Bivariant diagrams of major (SiO_2, FeO_T, Al_2O_3 and TiO_2) and trace (Rb, Ba, Sr, La, U and Th) elements vs. MgO.

The additional normalization of the incompatible elements to Ti = 1, showed on Figure 10D, assists the visualization of the effects of crustal contamination (segment A), source composition and degree of partial melting (segment B) and depth of melt generation (segment C) (Pearce, 2008). The samples show some crustal contamination of the magma, which has its origin in an enriched source with low degree of partial melting and at high depths (Fig. 10D). Since the other proxies do not show crustal contamination, this could be due sourcing from an already metasomatized mantle. The behavior of average composition of Paranapanema samples that did not suffer crustal contamination (based on initial Sr isotope ratios < 1) (Marques et al. 2017) is slightly different, showing a higher enrichment source with lower melt degree and higher depths than this work samples. Altough the Th_N show high values, it is not possible to interpret this as a result of crustal contamination, since the $(Rb/Ba)_{PM}$ ratios point the opposite.

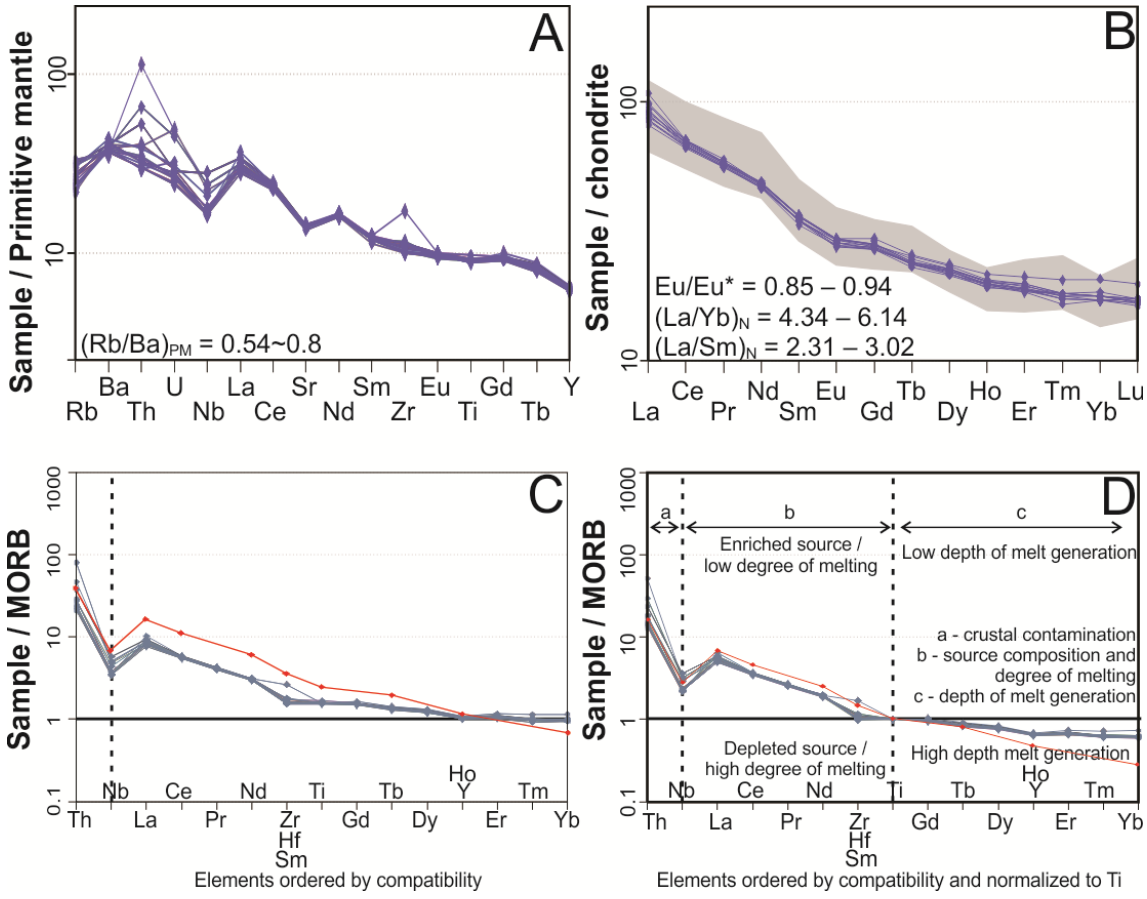

Figure 10 – A – Minor and trace elements normalized to the primitive mantle (Sun & McDonough, 1989). B – REE normalized to chondrite (Sun & McDonough, 1989). Gray field represent the Paranapanema type basalts, with data from Pinto & Hartmann (2011). C – Incompatible elements normalized to MORB (Sun & McDonough, 1989). D – Incompatible elements normalized to MORB (Sun & McDonough, 1989) and to Ti = 1. The red line represents the average sample composition of Paranapanema samples that did not suffer crustal contamination (based on initial Sr isotope ratios < 1) (Marques et al. 2017).

The average composition of the Água Vermelha basalts, however shows some differences from the average composition of other Paranapanema rocks, with slightly lower contents of SiO_2, TiO_2, Fe_2O_3, K_2O and P_2O_5 and higher contents of MgO, CaO and Na_2O compared to the samples from Rocha-Junior et al. (2013), Machado et al., (2017) and Pinto & Hartmann (2011) (Fig. 11).

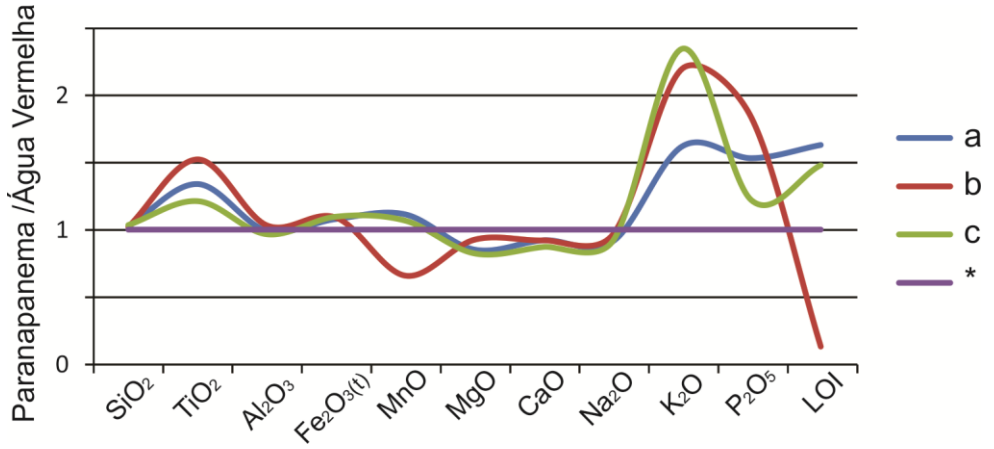

Figure 11 – Comparative chart between Paranapanema average compositions normalized to the average composition samples from this work (*). (a) Rocha-Junior et al. (2013), 10 samples; (b) Machado et al. (2007), 2 samples; (c) Pinto & Hartmann (2011), 14 samples.

6. MINERAL CHEMISTRY

The analysis of the lava flows (003b and 022) and basal flows (006, 023 and 027) samples, their chemical composition and variations of each mineral phase of the studied rocks are shown and discussed in this topic. The core and rim of the crystals of plagioclase and clinopyroxene and microlites of plagioclase, pyroxene and titanomagnetite were analyzed.

6.1.Plagioclase

The plagioclases were classified according to the Or-Ab-An diagram (Deer et al., 2003) (Fig. 12). Plagioclase microlites from both lava and basal flows are composed of andesine, with anorthite (An), albite (Ab) and orthoclase (Or) contents between $An_{59}Ab_{39}Or_2$ and $An_{67}Ab_{32}Or_1$. The phenocrysts from the lava and basal flows show a very weak compositional zoning (see table 3). The chemical formula for the phenocrysts of the lava flow can be summarized as $An_{80}Ab_{19}Or_1$ and is characterized as bytownite. There are two distinct groups of phenocrysts on the basal flow, with a slightly different composition from rim to core, being the first group characterized as bytownite

($An_{81}Ab_{18}Or_1$ to $An_{70}Ab_{29}Or_1$) and the second group as labradorite ($An_{69}Ab_{30}Or_1$ to $An_{64}Ab_{34}Or_2$). Table 3 summarizes the data of plagioclases analysis.

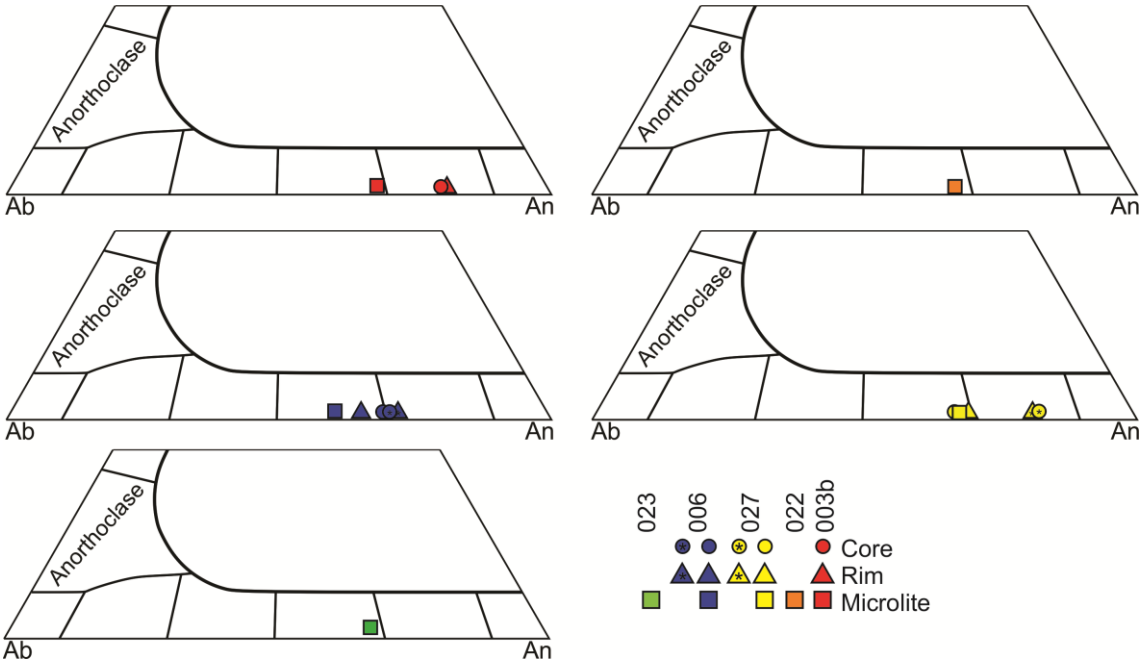

Figure 12 – Ternary diagram plot (Or-Ab-An) (Deer et al., 2003) for plagioclases from samples of the ring structure E6. Circle = core, triangle = rim, square = microlite.

Table 3 – Summary of plagioclase data from samples of the ring structure E6. Or=orthoclase, Ab=albite, An=anorthite

	Sample	Cristal	%Or	%Ab	%An	Mineral
Lava flow	***003b***	Microlite	1	31	67	Labradorite
		Phenocryst - core	1	20	80	Bytownite
		Phenocryst - rim	1	20	80	Bytownite
	22	Microlite	1	33	66	Labradorite
Basal flow	***6***	Microlite	2	39	59	Labradorite
		Phenocryst - core	1	30	69	Labradorite
		Phenocryst - rim	1	34	64	Labradorite
		Phenocryst - core	1	30	69	Bytownite
		Phenocryst - rim	1	29	70	Bytownite
	27	Microlite	1	32	67	Labradorite
		Phenocryst - core	1	18	81	Bytownite
		Phenocryst - rim	1	19	80	Bytownite
		Phenocryst - core	1	33	66	Labradorite
		Phenocryst - rim	1	31	68	Labradorite
	23	Microlite	1	32	67	Labradorite

6.2.Pyroxene

The clinopyroxene found in the samples is classified as augite in the Wo-En-Fs diagram of Morimoto (1988) (Fig. 13). The main features of the crystals are presented on Table 4.

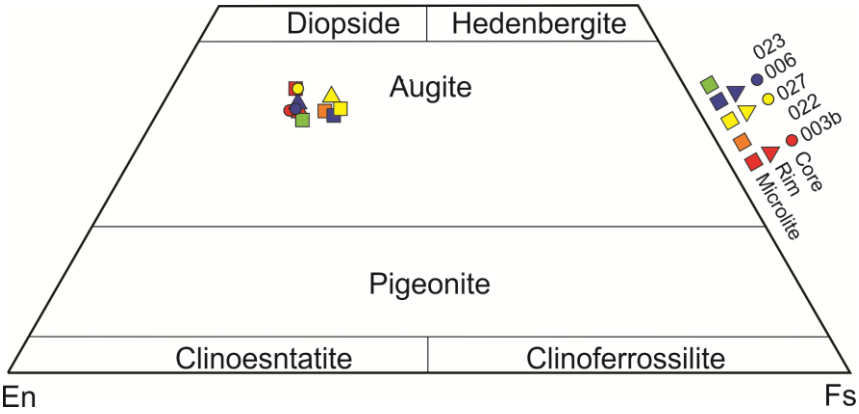

Figure 13 – Ternary diagram plot (Wo-En-Fs) (Morimoto, 1988) for clynopyroxenes from ringstructure E6. Circle = core, triangle = rim, square = microcrystal.

Table 4 – Summary of pyroxene data from samples of the ring structure E6. Fs=ferrossilite, En=enstatite, Wo=wollastonite.

	Sample	Crystal type	Chemical formula	%Fs	%En	%Wo
Lava flow	***003b***	Microlite	$(Ca_{0,76}Na_{0,01})(Mg_{0,90}Fe_{0,28}Ti_{0,02}Al_{0,02})(Si_{1,93}Al_{0,07})O_6$	14,34	46,59	39,07
		Phenocryst - core	$(Ca_{0,70}Na_{0,01})(Mg_{0,94}Fe_{0,29}Ti_{0,02}Al_{0,01})(Si_{1,89}Al_{0,11})O_6$	15,23	48,81	35,96
		Phenocryst - rim	$(Ca_{0,69}Na_{0,01})(Mg_{0,93}Fe_{0,32}Ti_{0,02}Al_{0,08})(Si_{1,93}Al_{0,07})O_6$	16,47	47,68	35,85
	022	Microlite	$(Ca_{0,70}Na_{0,01})(Mg_{0,87}Fe_{0,38}Ti_{0,03}Al_{0,02})(S_{i1,92}Al_{0,08})O_6$	19,34	44,80	35,86
Basal flow	***006***	Microlite	$(Ca_{0,70}Na_{0,01})(Mg_{0,86}Fe_{0,41}Ti_{0,02}Al_{0,01})(Si_{1,92}Al_{0,08})O_6$	20,76	43,75	35,49
		Phenocryst - core	$(Ca_{0,77}Na_{0,01})(Mg_{0,93}Fe_{0,29}Ti_{0,02})(Si_{1,9}Al_{0,1})O_6$	14,53	46,34	39,14
		Phenocryst - rim	$(Ca_{0,75}Na_{0,01})(Mg_{0,85}Fe_{0,37}Ti_{0,02})(Si_{1,91}Al_{0,09})O_6$	19,03	42,96	38,01
	027	Microlite	$(Ca_{0,70}Na_{0,01})(Mg_{0,82}Fe_{0,41}Ti_{0,03}Al_{0,03})(Si_{1,92}Al_{0,08})O_6$	21,10	42,48	36,42
		Phenocryst - core	$(Ca_{0,69}Na_{0,01})(Mg_{0,91}Fe_{0,30}Ti_{0,02}Al_{0,04})(Si_{1,92}Al_{0,08})O_6$	15,74	47,91	36,35
		Phenocryst - rim	$(Ca_{0,75}Na_{0,02})(Mg_{0,88}Fe_{0,28}Ti_{0,02}Al_{0,03})(Si_{1,92}Al_{0,08})O_6$	15,65	47,37	36,98
	023	Microlite	$(Ca_{0,68}Na_{0,01})(Mg_{0,93}Fe_{0,33}Ti_{0,02}Al_{0,03})(Si_{1,91}Al_{0,09})O_6$	17,30	48,00	34,70

6.2.1. Pyroxene thermometry

Figure 14 shows the diagram plot for the analyzed samples and Table 5 summarizes the data. Sample 003b, coming from the lava flow number 4, shows phenocryst with higher crystallization temperature (1100º C) than microlites (1000 ºC), and slightly higher than the microlites of sample 022 (1080 ºC), coming from the lava flow number 1.

The basal flow samples show distinct data. The microlites from sample 023 yield the higher temperature of crystallization (1120 ºC). The phenocrysts from sample 006

have a core-rim crystallization temperature ranging from 1100 ºC to 1080 ºC while the microlites have the same crystallization temperature of the rim. The phenocrysts of the sample 027 have lower crystallization temperature (1000 ºC) than the microlites (1050 ºC).

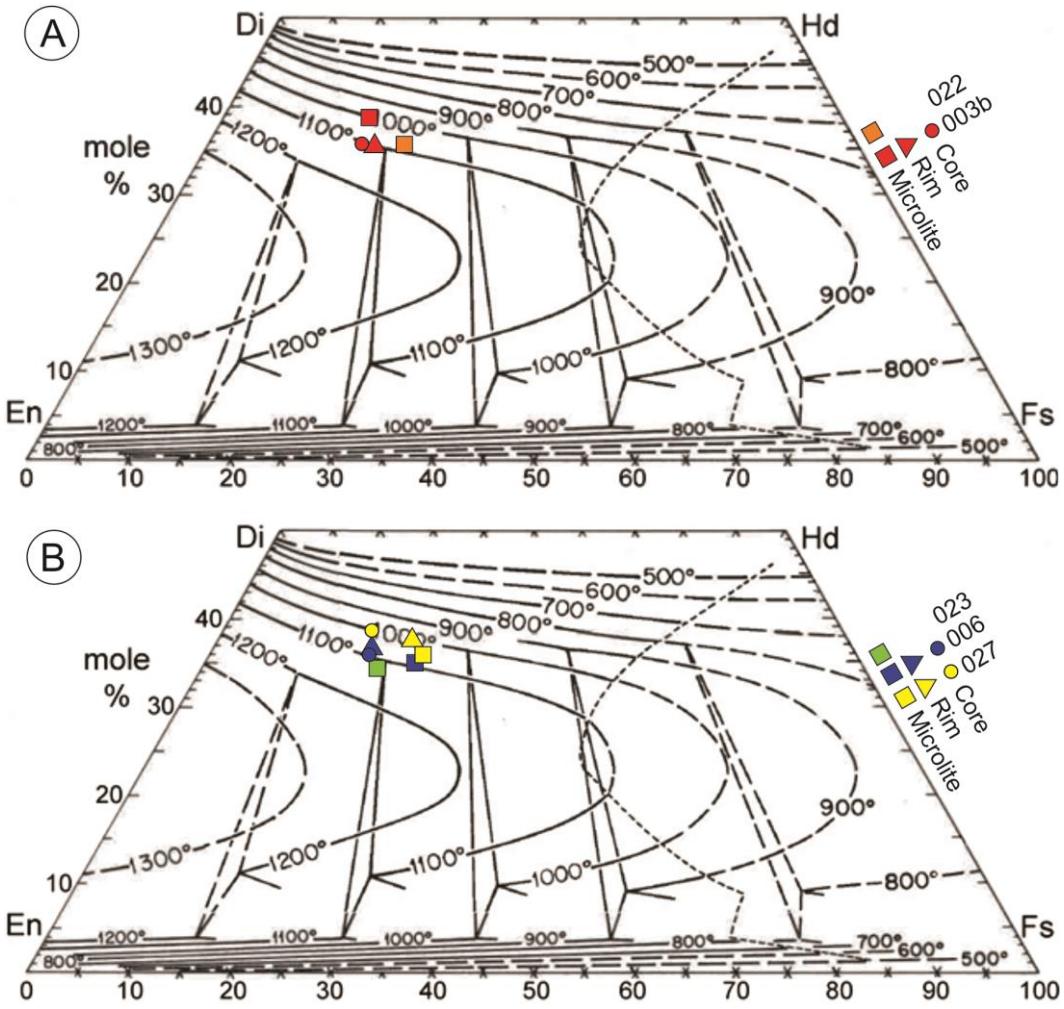

Figure 14 – Pyroxene thermometry based on Lindsley (1983). P = 1 atm. A – Lava flow; B – Basal flow.

Table 5 – Summary data for pyroxene thermometry from samples of the ring structure E6.

	Sample	**Crystal type**	**T (º C)**
Lava flow	***003b***	Microlite	1000 º C
		Phenocryst - core	1100 ºC
		Phenocryst - rim	1100 ºC
	22	Microlite	1080 ºC
Basal flow	***6***	Microlite	1080 ºC
		Phenocryst - core	1100º C
		Phenocryst - rim	1080 ºC
	27	Microlite	1050 ºC
		Phenocryst - core	1000 ºC
		Phenocryst - rim	1000 ºC
	23	Microlite	1120 ºC

6.3.Titanomagnetite (ulvöspinel)

The oxide analyses were plotted on the ternary FeO vs. TiO_2 vs. Fe_2O_3 diagram (Akimoto & Katsura, 1959). Since the microanalysis considered only FeO, the estimates of FeO and Fe_2O_3 were made as described in the Materials and Methods section. This diagram shows the major solid solution series magnetite-ulvöspinel, hematite-ilmenite and ferropseudobrookite-pseudobrookite (Fig. 15A). The skeletal oxides (Fig. 15B) analyzed for both lava and basal flows plots on the solid solution series of magnetite-ulvöspinel (titanomagnetite), and are close to the ulvöspinel end-member. Table 5 summarizes the data for the titanomagnetite analysis.

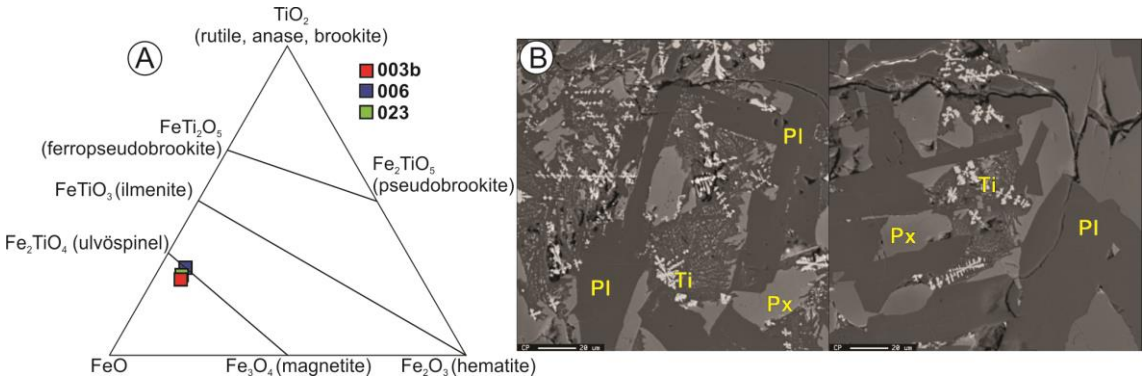

Figure 15 – A – Ternary FeO vs. TiO_2 vs. Fe_2O_3 diagram (Akimoto & Katsura, 1959). B – Backscattering electron image, showing titanomagnetite (Ti), plagioclase (Pl) and pyroxene (Px) from a basalt samples of the ring structure E6.

Table 6 – Summary for titanomagnetite data from samples of the ring structure E6.

	Samples	**% FeO**	**% Fe_2O_3**	**% TiO_2**
Lava Flow	***003b***	67,56	7,52	24,91
	006	64,49	7,18	28,33
Basal Flow	***023***	67,01	7,46	25,53

7. DISCUSSION

The petrography and whole-rock analyses show that the basalts of Água Vermelha present a subalkaline and tholeiitic signature due to the alkali and silica contents as well as the presence of normative olivine and enstatite (Machado et al., 2007). The BRS samples show their MgO content increases with the enrichment of silica, different from the other samples of Paranapanema-type basalts, while the content of TiO_2, K_2O and P_2O_5 stay constant with the increase of silica and is significantly lower than the samples used in comparison. Also, they present an enrichment of Al_2O_3

MgO, CaO and Na_2O related to other Paranapanema samples (Rocha Junior et al, 2013; Machado et al., 2007; Pinto & Hartmann, 2011). The samples used in comparison do not show any differentiation trend (Fig. 16).

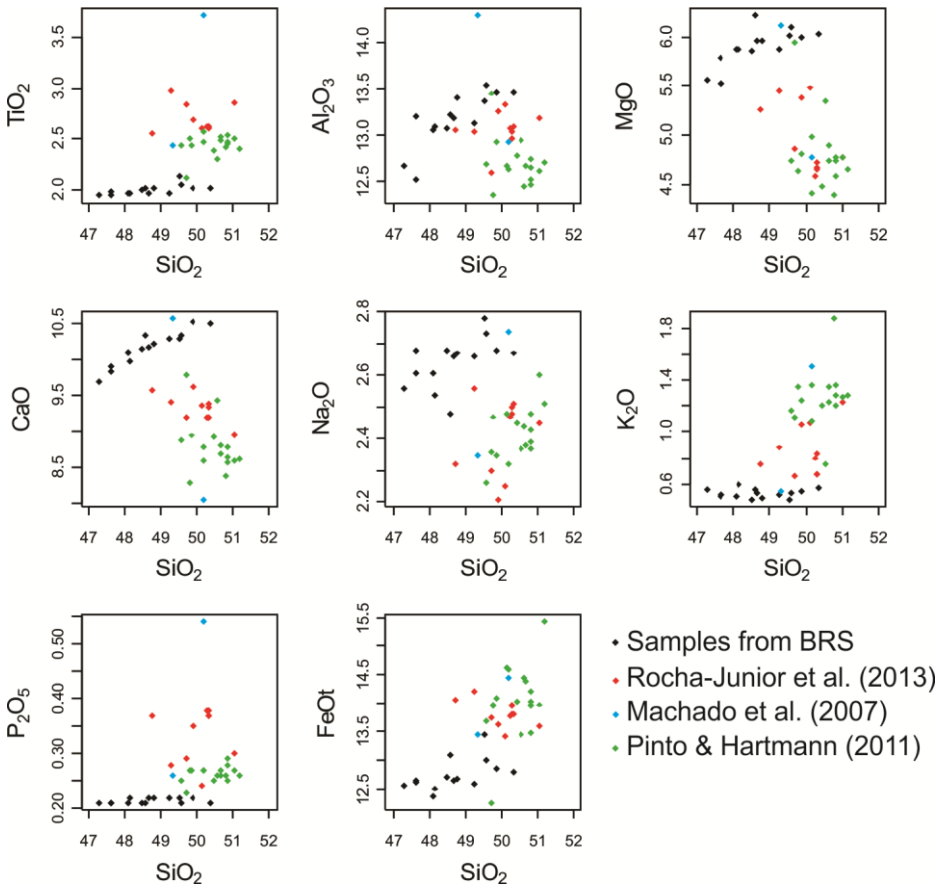

Figure 16 – Harker diagram of SiO_2 vs. major elements for samples of the ring structure E6 (BRS) as compared to other Paranapanema-types samples.

Through the mineral chemistry it was possible to determine that the plagioclase of both lava and basal flows has a composition ranging between bytownite and labradorite. The pyroxenes of the basal and lava flow are classified as augite. The pyroxene thermometry of the lava flow samples shows that they started to crystallize at 1100 ºC (core) and finished their crystallization at 1000 ºC (rim and microlite). However, the pyroxene thermometry of the basal flow shows that the microlites have a crystallization temperature equal or superior than the temperature of crystallization of the phenocrysts core. This and the plagioclase with slightly Ca-richer rim than the core suggest the possibility of new magma injections on the chamber.

The Eu anomaly is absent when the samples are normalized to the primitive mantle and is negative and subtle when normalized to the chondrite. This slight anomaly probably represents minor plagioclase fractionation. Moreover, the Sr anomaly

can be related to plagioclase fractionation, which is consistent with the presence of plagioclase phenocrysts and a glomeroporphyritic texture (Pinto & Hartmann, 2011). The negative Sr anomaly can be related to the enrichment of CaO with the increase of silica (Fig. 15).

The relatively high total REE content (Σ REE > 100 ppm) and the LREE and HREE ratios suggest some degree of contamination during the ascension through the continental crust, but due to the negative value of the $(Rb/Ba)_{PM}$ ratio, we can check that this contamination was not significant and we assume a fractional crystallization process responsible for these results. However, the increase of CaO and MgO related to the SiO_2 content cannot be explained by the fractional crystallization alone. Instead, the presence of the lava lake on the Água Vermelha BRS, with events of effusion and episodes of explosion (e.g. spatters), indicates new magma pulses on the shallow chamber, renovating the oxide contents. O'hara (1977) describes a model where the magma in a high-level chamber suffers continuous fractional crystallization and is periodically fed with new batch from the deep parental magma and, in this model, this influx displaces a portion of the residual liquid from the chamber as a lava flow. The rest of the previous magma mixes with the new batch and the fractionation process continues to occur. Also, a system that undergoes episodic recharge and eruption can develop distinctly different geochemical characteristics (Spera and Bohrson, 2004).

The analysis of the diagram proposed by Pearce (2008) suggests that the magma was originated in a high depth enriched source, with a low degree of melting. Marques et al. (1989) describes a garnet peridotite as a likely source for the basalts of the Paraná basin, as well as low partial melting of the HTi basalt sources, which is corroborated by the interpretations of the BRS evolution so far. The higher enrichment of LREE related to HREE, the LILE enrichment and the strong negative Nb anomalies are the main evidences of the involvement of metasomatized components (Rocha-Junior et al., 2013). According to those authors, the mantle was enriched in fluids and/or magma related to subduction processes during the Neoproterozoic, which hybridize the mantle peridotite with recycled components.

8. CONCLUSION

The rocks of the basaltic ring structure from Água Vermelha belong to the Paranapanema magma-type of the high titanium group of basalts from the Serra Geral Formation, but show some slight differences from other samples of the same magma-type in other places. The whole rock analyses show a subalkaline and tholeiitic signature.

Through the mineral chemistry it was possible to characterize the plagioclase, pyroxene and oxides of the samples analyzed. The plagioclases have a composition between bytownite and labradorite for both lava and basal flows. The clinopyroxenes are strictly augite. The pyroxene thermometry of the lava flow reveals that their crystallization started at 1100 ºC, with the phenocryst cores of sample 003b and microlites of sample 022, and finished at 1000 ºC with the phenocryst rims and microlites of sample 003b. On the other hand, the crystals of the basal flow have a different behavior, with a higher crystallization temperature of microlites compared to the phenocrysts. The oxides are characterized as titanomagnetite (ulvöspinel).

Through the whole rock analyses of the lava and basal flows it is possible to determine that the magma source has a high depth and low degree of partial melting. The magma on the shallow magmatic chamber suffered fractional crystallization and suffered new magma injections, which were responsible for the effusion of samples of the already differentiated magma. The remaining differentiated liquid mixed with the new batches during the evolution of the structure.

The singularities present in Água Vermelha – such as the presence of basaltic ring structures, unusual in PEMP – show the necessity of deeper studies at the region. Thus, the geochemical analyses as well as the geological mapping and stratigraphic study are important to progress on the geological comprehension of the Paraná-Etendeka Magmatic Province.

CONSIDERAÇÕES FINAIS

A estrutura circular descrita na região de Água Vermelha apresenta quatro tipos de basaltos diferentes. O central flow apresenta basaltos vesículo-amigdaloidais, contendo estruturas em corda, de degaseificação e spatter, registrando eventos explosivos e sendo caracterizado como um lago de lava. O basal flow apresenta basaltos maciços, sem disjunções colunares e contém geodos de quartzo centimétricos a decimétricos. Os lava flows apresentam basaltos maciços com disjunções colunares e mergulhos suaves para o exterior da estrutura, sendo caracterizados como lobos de pahoehoe do tipo P. O main ring dyke é representado por basaltos maciços com disjunções colunares que se encontram horizontalizadas ou com uma suave inclinação. Os diques apresentam mergulhos para o centro da estrutura circular e são caracterizados como condutos secundários.

Através da gravimetria foi possível identificar uma anomalia Bouger positiva regional e uma anomalia Bouger negativa local no centro da estrutura circular. A primeira é uma resposta à diferença de densidade das litologias encontradas na região em que os basaltos apresentam alta densidade, ao contrário dos sedimentos. A segunda pode ser devido à baixa densidade dos basaltos vesículo-amigdaloidais no centro da estrutura circular ou apenas um reflexo da topografia. Essa mesma anomalia foi descrita em estruturas circulares de Odessa, Washington (USA) e caracterizada como uma resposta à diferença de densidade dos materiais, sendo menor no centro da estrutura (Parks & Banami, 1971).

Essa estrutura circular é caracterizada como um conduto formado no estágio final do vulcanismo, após o resfriamento quase total do topo das fissuras. Modelos de colapso como os propostos por McKee & Stradling (1970) e Hodges (1978) são descartados, pois não apresentam semelhanças estruturais e petrográficas com a estrutura circular de Água Vermelha (artigo 1). O modelo aqui proposto apresenta 3 etapas: (1) ocorre o vulcanismo fissural e, a seguir, (2) ocorre resfriamento que sela o topo das fissuras, formando condutos centrais localizados (lagos de lava) e (3) o gás presente no magma é responsável pelo fraturamento radial e anelar encontrado na estrutura. Os fraturamentos anelares são aproveitados como condutos secundários (main ring dyke).

Petrograficamente os basaltos apresentam textura intergranular ou subofítica. Mineralogicamente apresentam plagioclásio, piroxênio, óxidos e iddingsita e, quando ocorrem amigdalas, elas podem ser preenchidas por zeólitas, calcita, calcedônia ou celadonita. Os plagioclásios se apresentam como ripas euédricas a subédricas, de tamanho inferior a 0,8 mm, com terminações em rabo de andorinha. Os piroxênios são granulares, de tamanho inferior a 0,2 mm. Ambos ocorrem como microfenocristais, geralmente apresentando textura glomeroporfirítica com cristais euédricos a subédricos de tamanho ente 1,0 e 2,0 mm. Os óxidos são menores que 0,1 mm e possuem hábitos cúbico, prismático ou esqueletal. A iddingsita ocorre como pseudomorfo da olivina.

A litoquímica mostra que as rochas presentes na estrutura circular de Água Vermelha são basaltos toleíticos/sub-alcalinos, do tipo Paranapanema. Apesar de ter alguns indícios de contaminação crustal, ela não foi significativa. Ainda é possível interpretar que as fontes mantélicas eram enriquecidas, com baixo grau de fusão parcial e em alta profundidade. O magma presente na câmara superficial sofreu cristalização fracionada e injeção de novos magmas, responsável pela efusão do magma já diferenciado e que se misturavam com o restante do magma já diferenciado.

Pela química mineral foi possível caracterizar a composição dos plagioclásios, piroxênios e óxidos. Os plagioclásios possuem composição variando de labradorita a bytownita para os lava flow e basal flow. Os clinopiroxênios são estritamente augita. A termometria dos piroxênios do lava flow mostra que a cristalização começou a 1100 ºC (registrado no centro de microcristais e em micrólitos) e terminou em 1000 ºC (registrado em bordas de microcristais e micrólitos). Já a termometria dos piroxênios do basal flow possui um comportamento diferente, com temperaturas de cristalização maiores para os micrólitos quando comparados com os fenocristais. Os óxidos são caracterizados como titanomagnetita (ulvöspinélio).

As características singulares presentes na região de Água Vermelha – como a presença de estruturas circulares – mostra a necessidade de estudos mais aprofundados na região. Assim, os estudos de mapeamento, estratigrafia, gravimetria, petrografia, litoquímica e química mineral da região são importantes para o avanço na compreensão geológica da Província Magmática Paraná-Etendeka.

REFERÊNCIAS BIBLIOGRÁFICAS

Almeida, F. F. M. (1986). Distribuição regional e relações tectônicas do magmatismo pós-paleozóico no Brasil. Revista Brasileira de Geociências, 16(4), 325-349.

Akimoto, S. I., & Katsura, T. (1959). Magneto-chemical study of the generalized titanomagnetite in volcanic rocks. Journal of geomagnetism and geoelectricity, 10(3), 69-90.

Araújo, J.S., Björnberg, A.J.S., Silva, R.F. Da, Soares, L. (1977). A Complex Structure in Basaltic Lava Flows at Água Vermelha Dam – SP – Brasil. In: The Geotechnics Of Struturally Complex Formations, Proceedings, Capri.

Araújo, J. S. (1982). Estruturas Circulares de Água Vermelha. Dissertação de Mestrado, IG-USP, S. Paulo, 79.

Araújo, J.S. & Hasui, Y. (1985). Estruturas Vulcânicas em Basaltos no Vale do Rio Grande, São Paulo/Minas Gerais. In: Simpósio Regional De Geologia, 5., 1985, SBG/SP, Atas, v. 1, 289-300.

Bellieni, G., Comin-Chiaramonti, P., Marques, L. S., Melfi, A. J., Piccirillo, E. M., Nardy, A. J. R., & Roisenberg, A. (1984). High-and low-TiO2 flood basalts from the Paraná plateau (Brazil): petrology and geochemical aspects bearing on their mantle origin. Neues Jahrbuch für Mineralogie Abhandlungen, 150, 273-306.

Bellieni, G., Comin-Chiaramonti, P., Marques, L.S., Melfi, A.J., Nardy, A.J.R., Papatrechas, C., Piccirillo, E.M., Roisenberg, A., Stolfa, D., (1986). Petrogenetic aspects of acid and basaltic lavas from the Paraná Plateau (Brazil): geological, mineralogical and petrochemical relationships. Journal of Petrology. 27, 915–944.

Burr, D. M., Bruno, B. C., Lanagan, P. D., Glaze, L. S., Jaeger, W. L., Soare, R. J., Tseung, J-M. W. B, Skinner Jr., J. A. & Baloga, S. M. (2009). Mesoscale raised rim depressions (MRRDs) on Earth: A review of the characteristics, processes, and spatial distributions of analogs for Mars. Planetary and Space Science, 57(5), 579-596.

Corner, B. (2000). Crustal framework of Namibia derived from magnetic and gravity data. Communications of the geological survey of Namibia, 12, 13-19

Courtillot, V. E., & Renne, P. R. (2003). On the ages of flood basalt events. Comptes Rendus Geoscience, 335(1), 113-140.

Deckart, K., Féraud, G., Marques, L. S., & Bertrand, H. (1998). New time constraints on dyke swarms related to the Paraná-Etendeka magmatic province, and subsequent South Atlantic opening, southeastern Brazil. Journal of Volcanology and Geothermal Research, 80(1-2), 67-83.

Deer, W.A., Howie, R.A., Zussman, J., (2003). An Introduction to the Rock-Forming Minerals. Longman Scientific and Technical, New York.

Ernesto M., Raposo M. I. B., Marques L. S., Renne P. R., Diogo L. A., De Min A. (1999). Paleomagnetism, geochemistry and 40Ar/39Ar dating of the North-eastern Paraná Magmatic Province: tectonic implications. Journal of Geodynamics, 28:321-340.

Faust, G. T. (1975). A review and interpretation of the geologic setting of the Watchung Basalt flows, New Jersey. Geological Survey, No. 864-A.

Frank, H. T., Gomes, M. E. B., & Formoso, M. L. L. (2009). Review of the areal extent and the volume of the Serra Geral Formation, Paraná Basin, South America. Pesquisas em Geociências, 36(1), 49-57.

Hall, A. (1987). Igneous petrology. Longman Scientific & Technical. Wiley.

Hodges, C. A. (1978). Basaltic ring structures of the Columbia Plateau. Geological Society of America Bulletin, 89(9), 1281-1289.

Hooper P.R. & Hawkesworth C.J. (1993). Isotopic and geochemical constraints on the origin and evolution of the Columbia River Basalt. Journal of Petrology, 34:1203-1246.

IBGE (Fundação Instituto Brasileiro de Geografia e Estatística), 2004. Rede Brasileira de Monitoramento Contínuo <http://www.ibge.gov.br>.

Jaeger, W. L., Keszthelyi, L. P., Burr, D. M., Emery, J. P., Baker, V. R., McEwen, A. S., & Miyamoto, H. (2005). Basaltic ring structures as an analog for ring features in Athabasca Valles, Mars. In 36th Annual Lunar and Planetary Science Conference, v. 36, 1886.

Janasi, V. A., de Freitas, V. A., & Heaman, L. H. (2011). The onset of flood basalt volcanism, Northern Paraná Basin, Brazil: A precise U–Pb baddeleyite/zircon age for a Chapecó-type dacite. Earth and Planetary Science Letters, 302(1), 147-153.

Jerram, D. A., & Bryan, S. E. (2015). Plumbing systems of shallow level intrusive complexes. Advances in Volcanology, Springer, 1-22.

Jerram, D. A., & Widdowson, M. (2005). The anatomy of Continental Flood Basalt Provinces: geological constraints on the processes and products of flood volcanism. Lithos, 79(3), 385-405.

Johannsen, A. (1931). A Descriptive Petrography Of The Igneous Rocks. Vol-I.

Lindsley, D. H. (1983). Pyroxene thermometry. American Mineralogist, 68(5-6), 477-493.

Le Maitre, R. W. (2002). Igneous rocks: A classification and glossary of terms; Recommendations of the IUGS subcommission on the Systematics of Igneous rocks. Cambridge University Press. 2nd edn.

MacDonald, G. A., & Katsura, T. (1964). Chemical composition of Hawaiian lavas. Journal of petrology, 5(1), 82-133.

Machado, F.B., Nardy, A.J.R., Oliveira, M.A.F. (2007). Geologia e aspectos petrológicos das rochas intrusivas e efusivas mesozoicas de parte da borda leste da bacia do Paraná no estado de São Paulo, Revista Brasileira de Geociências, 37(1), 64-80.

Maniesi V., Oliveira M. A. F. (1997). Petrologia das soleiras de diabásio de Reserva e Salto do Itararé, PR. Geochimica Brasiliensis, 11, 153-169.

Mantovani M.S.M., Cordani U.G., Roisenberg A. (1985). Geoquímica isotópica em vulcânicas ácidas da Bacia do Paraná e implicações genéticas associadas. Revista Brasileira de Geociências,15:61-65

Marques, L. S. (1988). Caracterização geoquímica das rochas vulcânicas da Bacia do Paraná: implicações petrogenéticas. 183p. Tese de Doutorado, Departamento de Geofísica, IAG-USP, São Paulo.

Marques, L. S. (2001). Geoquímica dos diques toleíticos da costa sul-sudeste do Brasil: contribuição ao conhecimento da Província Magmática do Paraná. Tese (Doutorado). São Paulo: IAG-USP.

Marques, L. S., & Ernesto, M. (2004). O magmatismo toleítico da Bacia do Paraná. In: Mantesso-Neto, V., Bartorelli, A., Carneiro, C. D. R., Brito-Neves, B. B. (Eds.), Geologia do Continente Sul-Americano: evolução da obra de Fernando Flávio Marques de Almeida (245-263). São Paulo: Beca.

Marques, L. S., Piccirillo, E. M., Bellieni, G., Figueiredo, A. M. G., & De Min, A. (2003). Caracterização geoquímica dos diques básicos mesozóicos de natureza toleítica da costa sulsudeste do Brasil. Congresso Brasileiro de Geoquímica, 9, 652-654. Belém: SBGq.

Marques, L. S., Rocha-Júnior, E. R. V., Babinski, M., Carvas, K. Z., Petronilho, L. A., & De Min, A. (2016). Lead isotope constraints on the mantle sources involved in the genesis of Mesozoic high-Ti tholeiite dykes (Urubici type) from the São Francisco Craton (Southern Espinhaço, Brazil). Brazilian Journal of Geology, 46, 105-122.

Marques, L. S., De Min, A., Rocha-Júnior, E. R. V., Babinski, M., Bellieni, G., & Figueiredo, A. M. G. (2017). Elemental and Sr-Nd-Pb isotope geochemistry of the Florianópolis Dyke Swarm (Paraná Magmatic Province): crustal contamination and mantle source constraints. Journal of Volcanology and Geothermal Research.

McKee, B. & Stradling, D. (1970). The sag flowout: a newly described volcanic structure. Geological Society of America Bulletin, 81(7), 2035-2044.

Melfi A.J., Piccirillo E.M., Nardy A.J. (1988). Geological and magmatic aspects of the Paraná Basin: an introduction. In: E.M. Piccirillo, A.J. Melfi (eds). The Mesozoic Flood Volcanism of the Paraná Basin: Petrogenetic and Geophysical Aspects (1-13). São Paulo: IAG-USP.

Milani, E. J. (1997). Evolução tectono-estratigráfica da Bacia do Paraná e seu relacionamento com a geodinâmica fanerozóica do Gondwana sul-ocidental. Tese (Doutorado). Porto Alegre: Universidade Federal do Rio Grande do Sul.

Milani, E. J. (2004). Comentários sobre a origem e evolução tectônica da Bacia do Paraná. In: Mantesso-Neto, V., Bartorelli, A., Carneiro, C. D. R., Brito-Neves, B. B. (Eds.), Geologia do Continente Sul-Americano: evolução da obra de Fernando Flávio Marques de Almeida (265-291). São Paulo: Beca.

Milani, E. J., Melo, J. H. G, Souza, P. A., Fernandes, L. A., & França, A. B. (2007). Bacia do Paraná. Boletim de Geociências da Petrobrás, 15(2), 265-287.

Mincato, R. L. (2000). Metalogenia dos elementos do grupo da platina com base na estratigrafia e geoquímica da Província Ígnea Continental do Paraná. Tese (Doutorado). Campinas: Instituto de Geociências, UNICAMP.

Miyashiro, A. (1975). Classification, characteristics, and origin of ophiolites. The journal of geology, 83(2), 249-281.

ModelVision (2013). ModelVision Magnetic & Gravity Interpretation System, Tensor Research.

Morimoto, N. (1988). Nomenclature of pyroxenes. Mineralogy and Petrology, 39(1), 55-76.

O'hara, M. J. (1977). Geochemical evolution during fractional crystallisation of a periodically refilled magma chamber. Nature, 266, 503-507.

Pacheco, F. E. R. C.; Caxito, F. A.; Moraes, L. C.; Marangoni, Y. R.; Santos, P. R. S; Pedrosa-Soares, A. C. (2017). Basaltic ring structures of the Serra Geral Formation at the southern Triângulo Mineiro, Água Vermelha region, Brazil. Journal Of Volcanology And Geothermal Research.

Parks, H. & Banami, A.M. (1971). Gravity survey of Columbia Plateau ring dikes. Eos Transactions 52 (5), 433.

Peate, D. W. (1997). The Paraná-Etendeka Province. Large igneous provinces: Continental, oceanic, and planetary flood volcanism, 217-245.

Peate, D. W., Hawkesworth, C. J., & Mantovani, M. S. (1992). Chemical stratigraphy of the Paraná lavas (South America): classification of magma types and their spatial distribution. Bulletin of Volcanology, 55(1), 119-139.

Pearce, J. A. (2008). Geochemical fingerprinting of oceanic basalts with applications to ophiolite classification and the search for Archean oceanic crust. Lithos, 100(1), 14-48.

Piccirillo, E. M., & Melfi, A. J. (1988). The Mesozoic flood volcanism of the Paraná basin: petrogenetic and geophysical aspects: IAG-USP. São Paulo, 600pp.

Piccirillo E.M., Comin-Chiaramonti P., Melfi A.J., Stolfa D., Bellieni G., Marques L.S., Giaretta A., Nardy A.J.R., Pinese J.P.P., Raposo M.I.B., Roisenberg A. (1988). Petrochemistry of continental flood basalt-rhyolite suites and intrusives from the Paraná Basin (Brazil). In: E.M. Piccirillo, A.J. Melfi (eds). The Mesozoic Flood Volcanism of the Paraná Basin: Petrogenetic and Geophysical Aspects (107-156). São Paulo: IAG-USP.

Pik, R., Deniel, C., Coulon, C., Yirgu, G., & Marty, B. (1999). Isotopic and trace element signatures of Ethiopian flood basalts: evidence for plume–lithosphere interactions. Geochimica et Cosmochimica Acta, 63(15), 2263-2279.

Pilkington, M. & Grieve, R.A.F. (1992). The geophysical signature of terrestrial impact craters. Reviews of Geophysics., 30 (2): 161-181.

Pinto, V. M., & Hartmann, L. A. (2011). Flow-by-flow chemical stratigraphy and evolution of thirteen Serra Geral Group basalt flows from Vista Alegre, southernmost Brazil. Anais da Academia Brasileira de Ciências, 83(2), 425-440.

Pinto, V. M., Hartmann, L. A., Santos, J. O. S., McNaughton, N. J., & Wildner, W. (2011). Zircon U–Pb geochronology from the Paraná bimodal volcanic province support a brief eruptive cycle at~ 135Ma. Chemical Geology, 281(1), 93-102.

Pires, E. F., Guerra-Sommer, M., dos Santos Scherer, C. M., dos Santos, A. R., & Cardoso, E. (2011). Early Cretaceous coniferous woods from a paleoerg (Paraná Basin, Brazil). Journal of South American Earth Sciences,32(1), 96-109.

Renne, P. R., Ernesto, M., Pacca, I. G., Coe, R. S., Glen, J. M., Prévot, M., & Perrin, M. (1992). The age of Paraná flood volcanism, rifting of Gondwanaland, and the Jurassic-Cretaceous boundary. Science, 258(5084), 975-979.

Renne, P. R., Glen, J. M., Milner, S. C., & Duncan, A. R. (1996). Age of Etendeka flood volcanism and associated intrusions in southwestern Africa. Geology, 24(7), 659-662.

Scherer, C. M., & Goldberg, K. (2007). Palaeowind patterns during the latest Jurassic–earliest Cretaceous in Gondwana: Evidence from aeolian cross-strata of the Botucatu Formation, Brazil. Palaeogeography, Palaeoclimatology, Palaeoecology, 250(1), 89-100.

Seer, H. J.. Moraes, L. C., & Carneiro, M. A. (2011). Geologia e litogeoquímica dos diques toleíticos ATi vinculados aos lineamentos magnéticos de direção NW do Arco do Alto Paranaíba em Abadia dos Dourados, MG. SBG, Simp. Vulcanismo e Ambientes Associados, V, Resumos–CD-Rom.

Self, S., Keszthelyi, L., & Thordarson, T. (1998). The importance of pahoehoe. Annual Review of Earth and Planetary Sciences, 26(1), 81-110.

Spera, F. J., & Bohrson, W. A. (2004). Open-system magma chamber evolution: An energy-constrained geochemical model incorporating the effects of concurrent eruption, recharge, variable assimilation and fractional crystallization (EC-E′ RAχFC). Journal of Petrology, 45(12), 2459-2480.